

~~CONFIDENTIAL~~Copy
RM E53B04

6

APR 9 1953



RESEARCH MEMORANDUM

EFFECT OF FUEL INJECTORS AND LINER DESIGN ON PERFORMANCE
OF AN ANNULAR TURBOJET COMBUSTOR WITH VAPOR FUEL

By Carl T. Norgren and J. Howard Childs

Lewis Flight Propulsion Laboratory
Cleveland, Ohio

CLASSIFICATION CHANGED

To UNCLASSIFIEDBy authority of *NASA memo* Dated *Febr 18, 1963,*
s/ Boyd C. Myers II.
HRK - 4-30-63

CLASSIFIED DOCUMENT

This material contains information affecting the National Defense of the United States within the meaning of the espionage laws, Title 18, U.S.C., Secs. 793 and 794, the transmission or revelation of which in any manner to an unauthorized person is prohibited by law.

NATIONAL ADVISORY COMMITTEE
FOR AERONAUTICS

WASHINGTON

April 6, 1953

~~CONFIDENTIAL~~NACA LIBRARY
LANGLEY AERONAUTICAL LABORATORY
Hampton, Va.

NATIONAL ADVISORY COMMITTEE FOR AERONAUTICS

RESEARCH MEMORANDUM

EFFECT OF FUEL INJECTORS AND LINER DESIGN ON PERFORMANCE OF

AN ANNULAR TURBOJET COMBUSTOR WITH VAPOR FUEL

By Carl T. Norgren and J. Howard Childs

SUMMARY


A direct-connect duct investigation was conducted with a one-quarter segment of a $25\frac{1}{2}$ -inch-diameter annular combustor which had been previously developed for liquid fuel injection. This combustor was modified by changing the fuel injectors and the liner design for vapor fuel injection. A total of 11 fuel injection schemes and 2 liner air-entry hole patterns were investigated as well as a liner designed for low pressure drop. Values quoted subsequently for simulated flight performance refer to operation of the combustor in a typical 5.2 pressure ratio turbojet at a flight Mach number of 0.6.

The combustor giving highest combustion efficiencies (model 14I) produced efficiencies above 98 percent at altitudes up to 61,000 feet at cruise (85 percent rated) engine speed. Increasing the air flow rate through this combustor to a value 69 percent above current design practice resulted in no appreciable effect on combustion efficiency at 56,000 feet at cruise speed. However, the outlet temperature profile for this combustor was unsatisfactory, and the pressure drop through the combustor was approximately twice as great as for many production-model combustors.

The combustor designed for low pressure drop (model 15I) gave a pressure drop only 60 percent of that for model 14I, but the combustion efficiency of this combustor was low. The data indicate that combustion efficiency could be improved by a liner design change to increase the amount of air entering the primary combustion zone.

INTRODUCTION

A general research program is in progress at the NACA Lewis laboratory to determine design criteria for turbojet combustors. One objective of this general program is the development of combustors that operate efficiently at lower pressures and at higher air flow rates, as



pointed out in reference 1. The experimental combustor described in reference 1 operated with a higher combustion efficiency at severe conditions when using vapor fuel than when using liquid fuel despite the fact that the combustor was originally developed to obtain high performance with liquid fuel. No attempt was made in reference 1 to optimize the combustor design for handling vapor fuel.

The research reported herein is a continuation of the work of reference 1. The first objective of the research was to improve the combustor of reference 1 to obtain higher combustion efficiencies with vapor fuel. The second objective was to reduce the combustor pressure loss, since the total-pressure loss through the combustor of reference 1 was approximately twice as high as the pressure losses obtained with several production model combustors.

A direct-connect duct investigation was conducted with a one-quarter segment of a 25 $\frac{1}{2}$ -inch-diameter annular turbojet combustor using vapor fuel. The data obtained with vapor fuel are believed to be representative of the performance to be expected when a fuel vaporizer is incorporated into the combustor. The initial combustor configuration was identical with the combustor of reference 1. The fuel injectors and the air-entry holes in the combustor liner were altered so that the combustor was better adapted for operation with vapor fuel. A total of 11 fuel injection schemes and 2 air-entry hole patterns were investigated. A new combustor liner designed for low pressure drop was also included in this investigation.

The operating conditions investigated included low pressure conditions typical of high-altitude, reduced-throttle flight and air flow rates per unit combustor frontal area which are typical of current engine design practice and 69 percent above current practice. The data presented include combustion efficiencies, pressure losses, and combustor-outlet temperature profiles over a range of fuel-air ratios. The performance data are compared with similar data for the combustor of reference 1.

APPARATUS

Installation and Instrumentation

The combustor installation and instrumentation were identical with those of reference 1. A diagram of the combustor installation is shown in figure 1. The combustor-inlet and combustor-outlet ducts were connected to the laboratory air supply and low-pressure exhaust systems, respectively. Air flow rates and combustor pressures were regulated by remote-controlled valves located upstream and downstream of the combustor. The combustor inlet-air temperature was controlled by an electric heater.

Air flow was metered by a concentric-hole, sharp-edge orifice installed according to A.S.M.E. specifications. The vapor fuel flow rate was metered by a calibrated sharp-edge orifice. Thermocouples and pressure tubes were located at the combustor-inlet and -outlet planes indicated in figure 1. The number, type, and position of these instruments at each of the planes are indicated in figure 2. The combustor-outlet thermocouples were located at centers of equal areas in the duct. Pressure tubes were connected to absolute manometers; thermocouples, to a recording potentiometer.

The fuel used in this investigation was vaporized commercial propane from the laboratory distribution system.

Combustors

Each combustor was designed to fit into the same combustor housing, which consisted of a $1/4$ segment of a single-annulus combustor having an outside diameter of $25\frac{1}{2}$ inches, an inside diameter of $10\frac{5}{8}$ inches, and a length from fuel atomizers to combustor-outlet thermocouples of approximately 23 inches. The maximum combustor cross-sectional area was 105 square inches (corresponding to 420 sq in. for the complete combustor).

A total of three combustor liners was investigated. The first of these liners, model 13, was identical with the combustor of reference 1. A cutaway view of the model 13 liner installed in the combustor housing is presented in figure 3; figure 4 shows a longitudinal cross-sectional view of this liner; and figure 5 shows the arrangement of the air-entry holes in the liner.

The model 14 liner resulted from design modifications to better adapt the combustor for handling vapor fuel. This liner (fig. 6) differed from the model 13 liner in two important respects: (1) the air-entry holes at the upstream end of the liner were larger; and (2) the radiation shield, which protects the fuel injectors from flame radiation, was perforated to admit air into the combustion zone in an axial direction.

The details of the model 15 liner, which was designed to give low pressure drop, are presented in figure 7. The walls of the liner did not diverge as did those of models 14 and 15. The air-entry holes in the walls of the model 15 liner were identical with those in model 13.

The fuel injectors were located in a manifold at the upstream end of the combustor and injected fuel in the downstream direction. Some of the combustors reported herein utilized 10 fuel injectors, while others

utilized only 5 fuel injectors. To permit operation with either 5 or 10 fuel injectors, a dual manifold (shown in fig. 8) was used. The various fuel injectors which were used in this investigation are shown in figure 9. These fuel injectors were designed to produce various fuel distribution patterns.

A total of 11 fuel injector configurations and 3 combustor liner configurations was investigated; these are tabulated and described in table I. Each combustor is given a numerical designation to indicate the liner configuration (13, 14, or 15) followed by a letter designation to indicate the fuel injector design.

PROCEDURE

Combustion efficiency and combustor total-pressure loss data were recorded for a range of fuel-air ratios at the following conditions:

Test condition	Combustor inlet total pressure, P_1 , in. Hg abs	Combustor inlet total temperature, T_1 , $^{\circ}\text{F}$	Air flow rate per unit area, W_a/A_r , lb/(sec)(sq ft)	Simulated flight altitude in reference engine, cruise speed
A	15	268	2.14	56,000
B	8	268	1.14	70,000
C	5	268	.714	80,000
E	15	268	3.62	56,000

These conditions simulate operation of the combustor in a reference turbojet engine which is a typical 5.2 pressure ratio turbojet operating at a Mach number of 0.6. The cruise speed of the engine is assumed to be 85 percent of the rated rotor speed. Test conditions A through C require air flow rates per unit combustor frontal area which are typical of current turbojet engines. Test condition E requires an air flow rate which is 69 percent above current practice.

Combustion efficiency was computed as the percentage ratio of actual to theoretical increase in enthalpy from the combustor-inlet to the combustor-outlet instrumentation planes using the method of reference 2. For calculation of combustor-outlet enthalpy, the temperature was computed as the arithmetic mean of the 30 outlet thermocouple indications for most of the data presented herein. For a limited number of data points the average combustor-outlet temperature was computed from the relation

$$T_{av} = \frac{\sum_{n=1}^{n=30} m_n T_n}{\sum_{n=1}^{n=30} m_n}$$

which allows for differences in mass flow at the various thermocouple locations. In this equation, T_{av} is the average outlet temperature, T_n is the temperature indication of a single one of the 30 outlet thermocouples, and m_n is the mass flow rate through the portion of the duct in which this thermocouple is located. No corrections were made for radiation or velocity effects on the thermocouple indications.

2837 Combustor reference velocities were computed from the air mass flow rate, the combustor-inlet density, and the maximum combustor cross-sectional area (105 sq in.). The total-pressure loss was computed as the dimensionless ratio of the total-pressure loss to the combustor reference dynamic pressure. The radial distribution of temperatures at the combustor outlet was determined at each test condition investigated and at two values of combustor temperature rise (approximately 680° and 1180° F, the required values at 85 and 100 percent rated speed in the reference turbojet engine at altitudes above the tropopause). The temperature at each of the five radial positions was computed as the average of four thermocouple readings at that radial position (see fig. 2(b)). The temperature rake at each side wall of the combustor was not included in these average temperatures since the side walls exerted an influence on the flow pattern and the temperature profile which would not be obtained in a full combustor annulus.

RESULTS AND DISCUSSION

The experimental data obtained in the direct-connect duct investigation of a one-quarter segment of a 25 $\frac{1}{2}$ -inch annular turbojet combustor with various fuel injectors and liner configurations are presented in table II.

Accuracy and Reproducibility

Figure 10 shows values of combustion efficiency obtained with the model 13A combustor at test conditions B and C. The data from reference 1 show values of combustion efficiency obtained prior to the beginning of the investigation reported herein. Combustion efficiencies obtained in check tests with this same combustor near the conclusion of the investigation reported herein are also shown in the figure. The combustion efficiencies obtained near the conclusion of this investigation average approximately 5 percent higher than the values obtained at the beginning of the investigation.

Figure 11 compares the radial distribution of outlet temperatures obtained with the model 13A combustor in reference 1 and in the check tests with this same combustor near the conclusion of this investigation.

The combustor-outlet temperature profiles obtained in this investigation were more uneven than those obtained in reference 1. Progressive warping of the liner is believed to have caused this effect. Previous experience has shown that as the outlet temperature distribution becomes more uneven, the mass flow per unit area also becomes more uneven, with the mass flow per unit area varying inversely as the value of temperature. This means that an average combustor-outlet temperature computed from the arithmetic mean of the various thermocouple indications would be erroneously high in those cases where the temperature profile was very uneven. Consequently, the combustion efficiencies of reference 1 are believed to be reasonably accurate; whereas those obtained near the conclusion of the investigation are believed to be high because of the nonuniform outlet temperature profiles.

At a limited number of test conditions, total-pressure tubes were installed at the combustor outlet to measure the radial distribution of mass flow across the combustor outlet, and appropriate corrections were made to the thermocouple indications to allow for variations in mass flow by each thermocouple. The combustion efficiencies computed from these corrected values of outlet temperature were lower than those computed from the temperatures based on the simple arithmetic mean of the thermocouple indications. The following table shows a comparison of combustion efficiencies computed by these two methods for combustor 14I:

Test condition	Average outlet temperature, °F		Combustion efficiency	
	Uncorrected for flow distribution	Corrected for flow distribution	Uncorrected for flow distribution	Corrected for flow distribution
C	902	875	85.7	81.9
C	1140	1109	88.1	85.5
C	1340	1286	87.6	83.1
E	950	918	107.8	100.0

The combustion efficiencies reported herein are values which have not been corrected for mass-flow distribution except where otherwise noted; these uncorrected combustion efficiencies cannot be considered accurate, inasmuch as they may be too high by as much as 2.0 to 8 percent at the various test conditions. The values are nevertheless significant since they show the relative performance of various combustor designs, particularly for designs investigated near the same time during the program.

Combustion Efficiency

Effect of fuel injectors. - Values of combustion efficiency obtained with the model 13 combustor and various fuel injectors at test condition C

are shown in figure 12. The curves of figure 12 were taken from the appendix, which presents more detailed efficiency data for these various combustors. Only the data of figure 12 need be considered in comparing the performance of these combustors. This comparison shows that the highest combustion efficiencies were obtained throughout most of the fuel-air ratio range with combustor 13I. This combustor employed five fuel injectors, each consisting of a simple sharp-edge orifice (table I). The additional data of the appendix also show combustor 13I to be equal to, or better than, the various other combustors at the other test conditions investigated. Figure 13 shows a comparison of the combustion efficiencies obtained with the model 13I combustor with the efficiencies obtained with the model 13A combustor at test condition C. The data presented for the model 13A combustor are the data obtained near the conclusion of this investigation (fig. 10) rather than the data from reference 1. The data of figure 13 are therefore comparable for the two combustors, since they were investigated near the same time. The model 13I combustor gave efficiencies 3 to 6 percent above the efficiencies obtained with model 13A. This improvement in performance was obtained by modifying the fuel injectors so that they were better adapted for handling vapor fuel.

The simple orifices of the model 13I combustor provide much less spreading of the fuel than some of the other injectors investigated. The higher efficiency of the model 13I combustor may indicate that too much spreading of the fuel is not desirable.

Effect of air-entry holes. - Combustion efficiencies obtained with the model 14I combustor are presented in figure 14. The curve for the model 13I combustor is included for comparison. The model 14I combustor gave combustion efficiencies approximately 5 percent above those of the model 13I combustor throughout the range of fuel-air ratios at test condition C. This improvement in performance is the result of revising the liner air-entry holes for better operation with vapor fuel. Since only two liner air-entry hole patterns were investigated (models 13 and 14), the optimum air-entry hole pattern was not established.

A rough indication of whether further improvements in efficiency might be obtained by additional air-entry hole modifications was obtained by operating the model 14I combustor with air injection in five of the fuel injectors. During these tests, therefore, fuel and air entered the combustor through alternate fuel injectors. The total flow rate for the air injection was 0.042 pound per second. With air injection the model 14I combustor produced efficiencies approximately 5 percent above the values obtained in model 14I combustor with no air injection. This performance of the model 14I combustor with air injection may be indicative of the performance which may be obtainable with further changes in the liner air-entry holes.

Since the model 13A combustor was developed in reference 1 to give high performance with liquid fuel, the liner was near an optimum design for liquid fuel. The data obtained with the model 14I combustor therefore indicate that the liner air-entry hole arrangement should be quite different for vapor fuel and for liquid fuel. With vapor fuel injection, a greater portion of the total air should be entered through liner perforations near the upstream end of the combustor.

Summary of effect of several design variables. - The effects of some of the more important design variables on combustion efficiency are shown in the following table, which compares efficiencies at fixed operating conditions of four different combustors:

Description of combustor	Model	Combustion efficiency at test condition C; ΔT , 680° F
Combustor developed to give high efficiency with liquid fuel	13A	54 ^a
Same combustor using vapor fuel injected through liquid-fuel injectors	13A	76.5 ^a 79.5 ^b
Fuel injectors adapted for vapor fuel	13I	84.5 ^b
Liner air-entry holes adapted for vapor fuel	14I	89.5 ^b

^aData from reference 1.

^bThese values are high by about 3.5 percent.

Effect of liner shape. - Combustion efficiencies obtained with the model 15I combustor are presented in figure 15. The curve for the model 13I combustor is again included for comparison. The fuel injectors and the liner air-entry hole patterns were identical for these two combustors. The only difference between these combustors was the shape of the combustor liner. The model 15I combustor produced a much lower pressure drop through the combustor than did the model 13I combustor, as will be subsequently discussed. Because of the design changes utilized to obtain the lower pressure drop for the model 15I combustor, the air flow through each of the air-entry holes in the upstream end of the combustor would be expected to be less than the flow through these same holes in the model 13I combustor. It might be expected, therefore, that the primary zone of the model 15I combustor would operate fuel-rich. The data of figure 15 indicate this to be the fact, since the combustion efficiencies obtained with the model 15I combustor are very much lower than the efficiencies obtained with the model 13I combustor, particularly at the

higher fuel-air ratios. The marked decrease in combustion efficiency accompanying an increase in fuel-air ratio, which is noted for the model 15I combustor, is believed typical of combustors which have a primary zone designed to operate fuel-rich.

From the foregoing considerations it would be expected that the efficiency of the model 15I combustor can be improved by additional air in the primary zone. This was accomplished by air injection through half the fuel nozzles. Two air injection rates were investigated, with the higher injection rate producing the highest efficiencies (fig. 15). With the higher rate of air injection the combustion efficiencies obtained with the model 15I combustor were only about 6 percent below those obtained with the model 13I combustor at the single high value of fuel-air ratio investigated. These results indicate that substantial improvements in combustion efficiency of the model 15I combustor may be effected by changing the design of the air-entry holes in the combustor liner.

Correlation of combustion efficiency on model 14I combustor. - The combustion efficiencies of the model 14I combustor, which gave the highest efficiencies of the various combustors investigated, are plotted in figure 16 as a function of the combustion parameter V_r/p_1T_1 (ref. 3). A similar correlation curve for the model 13A combustor from reference 1 is included for comparison. The tailed symbols in figure 16 indicate data corrected for flow distribution. The curve is drawn through the corrected data points for the standard velocity conditions (test conditions A and C). As previously mentioned, the data of reference 1 are believed to be correct, so the curves for the two combustors are comparable. The correlation is presented for a single value of combustor temperature rise, 680° F, which is the value of temperature rise required for operation at 85 percent rated speed at altitudes above the tropopause. This value of required temperature rise was obtained from engine performance curves which were extrapolated to the higher altitude conditions by assuming constant efficiencies of engine components other than the combustor.

The comparison in figure 16 shows that model 14I combustor produced combustion efficiencies as much as 9 percent above those obtained with the model 13A combustor at severe operating conditions.

Estimated flight performance. - Figure 17 presents the estimated combustion efficiency (corrected values) of the model 14I combustor at various flight conditions in the reference turbojet engine; these curves were obtained by using the data of figure 16. For each value of combustion efficiency, the value of the combustion parameter was read from the curve of figure 16. The flight altitude and engine speed producing each of these values of the combustion parameter were next determined from the engine performance curves for the reference engine.

These flight altitudes and engine speeds were then plotted to give the constant-efficiency lines of figure 17.

The curves of figure 17 are limited to the range of engine speeds from 80 to 100 percent rated speed. For this range of engine speeds the required combustor temperature rise varied from 550° to 1180° F and the combustion efficiency varied less than 3 percent for this range of combustor temperature rise. The use of figure 16, which was derived for a single value (680° F) of temperature rise, is therefore valid for this limited range of engine speed.

The two data points in figure 17 at 85 percent rated speed represent actual experimental data for the test conditions simulating flight operation at the conditions indicated on the figure. The combustion efficiencies listed beside each of these two data points match well with the values expected from interpolation between the curves of figure 17. The curves of figure 17 show that the model 14I combustor operated at efficiencies above 98 percent up to a simulated altitude of 61,000 feet at cruise (85 percent-rated) engine speed.

High air flow rates. - Figure 18 shows values of combustion efficiency obtained with the model 14I combustor at air flow rates typical of current practice and 69 percent above current design practice. At these test conditions ($P_1 = 15$ in. Hg and $T_1 = 268^{\circ}$ F, simulating operation of the combustor in the reference engine at 56,000 feet and 85 percent rated speed), no detrimental effect on combustion efficiency was noted over most of the range of fuel-air ratios as a result of increasing the air flow rate.

The data of figure 18, showing no marked effect on combustion efficiency due to an increase in air flow rate (velocity) of 69 percent, are not in accord with the correlation of figure 16. For this increase in velocity of 69 percent, figure 16 indicates that a decrease in combustion efficiency of 5 percent should occur. Since this decrease did not occur, the data point for test condition E in figure 16 falls about 5 percent above the curve. This discrepancy indicates that the parameter V_r/P_1T_1 does not properly allow for the effect of velocity on this particular combustor.

Combustor-Outlet Temperature Profiles

Figure 19 shows typical distributions of temperatures at the combustor outlet for the model 14I and 15I combustors. The radial distribution of temperatures with the model 14I combustor (fig. 19(a)) was much less uniform than the values obtained in reference 1; a curve for the model 13A combustor from reference 1 is included in figure 19(a) for comparison. The model 14I combustor employed the same secondary zone

air-entry hole pattern as did the model 13A combustor, and reference 1 pointed out that the outlet temperature profile was determined primarily by the arrangement of secondary air-entry holes in this combustor. The difference in temperature profiles noted for these two combustors is therefore believed to be caused primarily by the warping of the combustor liner, which occurred gradually throughout the test program reported herein.

The outlet temperature profiles obtained with model 14I combustor were not considered satisfactory, since they deviate markedly from the desired temperature distribution indicated by the dashed line in figure 19(a). The temperature distribution obtained with the model 15I combustor (fig. 19(b)) also deviates widely from the desired pattern of temperatures; no attempt was made in the investigation reported herein to remedy this temperature profile by combustor design changes.

Pressure Losses

The total-pressure drop through the combustors at test condition C for a range of density ratios (corresponding to a range of fuel-air ratios) is presented in figure 20. Since the measured pressure drop through the model 13 and model 14 combustors was the same as that reported in reference 1 for the model 13 combustor, a single curve from reference 1 is included in figure 20 to represent the pressure drop through these combustors. Experimental data are shown for the model 15I combustor. This combustor was designed for low pressure drop, and figure 20 shows that the pressure drop through the model 15I combustor was only 60 percent of the value for models 13 and 14. The pressure loss through the model 15I combustor compares favorably with the values obtained in many of the current production model combustors.

The lower pressure drop of the model 15I combustor was achieved by designing the liner so that the walls did not diverge as in previous models. This allowed a greater flow area for the air passing around the liner and entering the liner through the large secondary air-entry holes. It had been noted in appendix A of reference 1 that the high pressure drop of the previous combustor models was probably due to the flow restriction imposed on the secondary air in the flow passages outside the liner. The low pressure drop of the model 15I combustor serves to confirm this hypothesis.

SUMMARY OF RESULTS

An investigation was conducted in an annular turbojet combustor to improve combustion performance at low pressures and a high air flow rate. The design of fuel injectors, liner air openings, and liner geometries

was altered. The combustion efficiencies quoted in this section of the report have been corrected for mass flow distribution at the combustor outlet. The values quoted for simulated flight performance refer to operation of the combustor in a typical 5.2 pressure ratio turbojet engine at a flight Mach number of 0.6. The following results were obtained:

1. The combustor giving highest combustion efficiencies (model 14I) produced efficiencies above 98 percent at altitudes up to 61,000 feet at cruise (85 percent rated) engine speed. At conditions simulating cruise at 56,000 feet, no marked effect on performance resulted from increasing the air flow rate to a value 69 percent above current design practice. However, this combustor produced an unsatisfactory radial distribution of combustor-outlet temperatures, and the pressure loss was twice as great as the value encountered with many current production model combustors.

2. The combustor designed to produce low pressure drop (model 15I) gave a combustor pressure loss only 60 percent as great as that obtained with the model 14I combustor. However, the combustion efficiencies of this combustor were considerably lower than those obtained with model 14I. The data indicate that the model 15I combustor requires modification to increase the amount of air entering the primary zone of the combustor in order to improve combustion efficiencies above the values reported herein.

3. A comparison of the combustion efficiencies obtained at operating conditions simulating cruise at 80,000 feet with different combustors shows improvements obtained as a result of changing various design features as follows:

- (a) Increase in combustion efficiency of approximately 22 percent by changing from liquid to vapor fuel injection in a combustor (model 13A) which had been developed for liquid fuel
- (b) Additional increase in efficiency of 5 percent by changing the fuel injectors so that they were better adapted for handling vapor fuel (model 13I)
- (c) Additional increase in efficiency of 5 percent by changing the liner air-entry holes so that they were better adapted for vapor fuel (model 14I)

The over-all result of these modifications was to increase the combustion efficiency from 54 percent to 86 percent at this test condition.

Lewis Flight Propulsion Laboratory
National Advisory Committee for Aeronautics
Cleveland, Ohio

2837

APPENDIX - COMBUSTION EFFICIENCIES OF COMBUSTOR MODELS 13 AND 14
WITH VARIOUS FUEL INJECTORS

The combustion efficiencies obtained with the model 13 and model 14 combustors with various fuel injectors are presented in figures 21 and 22, respectively. The curves from figure 21 for test condition C were compared in figure 12 where model 13I was shown to provide the highest efficiencies over most of the fuel-air ratio range. Comparing the efficiencies of these combustors at other test conditions leads to the same conclusion; namely, combustor model 13I is equal to or better than the various other combustors of figure 21.

It was shown with combustor model 13 (figs. 21(e) and 21(f)) that combustion efficiency increased as the fuel injector orifice diameter was increased for the three orifice sizes investigated. It therefore appeared possible that a further increase in fuel orifice size might result in further gains in efficiency. This possibility was investigated by using larger orifices in the model 14 combustor (model 14K). The results are shown in figure 22, where the efficiencies of the model 14K combustor are compared with those of model 14I. The comparison indicates that a further increase in fuel orifice size was not beneficial.

REFERENCES

1. Norgren, Carl T., and Childs, J. Howard: Effect of Liner Air-Entry Holes, Fuel State, and Combustor Size on Performance of an Annular Turbojet Combustor at Low Pressures and High Air-Flow Rates. NACA RM E52J09, 1953.
2. Turner, L. Richard, and Bogart, Donald: Constant-Pressure Combustion Charts Including Effects of Diluent Addition. NACA Rep. 937, 1949. (Supersedes NACA TN's 1086 and 1655.)
3. Childs, J. Howard: Preliminary Correlation of Efficiency of Aircraft Gas-Turbine Combustors for Different Operating Conditions. NACA RM E50F15, 1950.

TABLE I. - SUMMARY OF CONFIGURATIONS INVESTIGATED



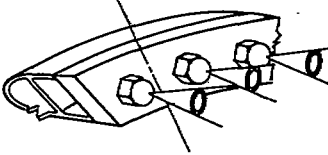
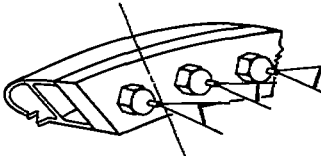
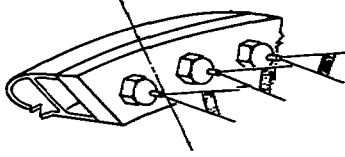
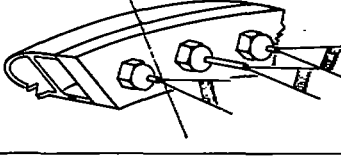
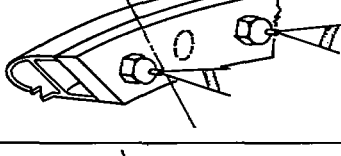
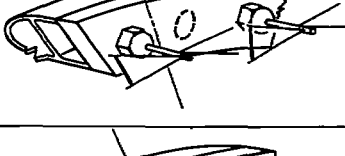

Modifi- cation	Combustor model	Number of fuel injectors		Description of injectors	Injector detail reference to fig. 9
1	13A	10		30 gal/hr, 60° swirl-type pressure atomizers; identical to model 13 combustor reported in ref. 1	9(a)
2	13B	10		Each injector consisted of a 0.01-in. wide slot designed to produce a fan-shaped jet of vapor fuel. Injectors were oriented so that vapor fans were in planes passing radially through center of combustor.	9(b)
3	13C	10		Injector similar in design to those of model 13B except slot width was increased and shape of slot was changed.	9(c)
4	13D	10		Fan injectors identical to those used in model 13C and extended fan injectors that injected fuel at a point approximately $1\frac{1}{2}$ in. downstream	9(c), 9(d)
5	13E	5		Fan injectors identical to those used in model 13C	9(c)
6	13F	5		Injectors were used with two slots oriented to produce a fan-shaped jet of vapor in planes at right angles to main axis of combustor.	9(e)
7	13G	5		Injectors similar to those used in model 13F, except fuel injection slots were located closer to upstream end of combustor.	9(f)

TABLE I. - SUMMARY OF CONFIGURATIONS INVESTIGATED - Concluded

NACA

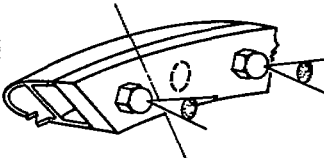
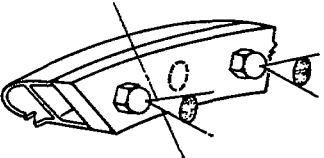
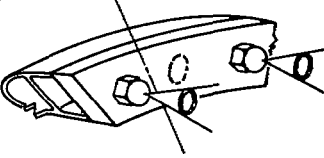
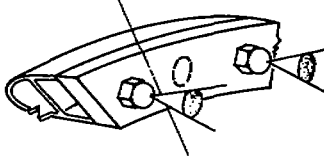
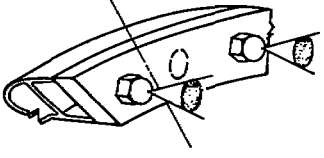
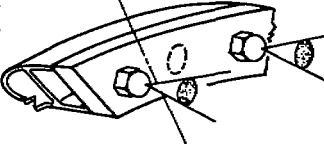
Modifi- cation	Combustor model	Number of fuel injectors		Description of injectors	Injector detail reference to fig. 9
8	13H	5		Injectors consisted of a simple sharp-edge orifice 5/64 in. in diameter.	9(g)
9	13I	5		Injectors consisted of a simple sharp-edge orifice 7/64 in. in diameter.	9(g)
10	13J	5		Injectors similar to those used in model 13I, except swirl generators were added in the injectors to give injector similar to standard swirl-type liquid atomizer.	9(h)
11	14I	5		Injectors identical to those used in model 13I	9(g)
12	14K	5		Injectors consisted of a simple sharp-edge orifice 1/8 in. in diameter.	9(g)
13	15I	5		Injectors identical to those used in model 13I	9(g)

TABLE II. - EXPERIMENTAL RESULTS



Run	Combustor-inlet total pressure, P_1 in. Hg	Combustor-inlet total temperature, T_1 or	Air flow rate, W_a lb/sec	Air flow rate per unit area, W_a/A_r lb/(sec) (sq ft)	Combustor reference velocity, V_r ft/sec	Fuel flow rate, W_f lb/hr	Fuel-air ratio, f	Mean combustor-outlet temperature, T_0 or	Mean temperature rise through combustor, ΔT_{Cp}	Combustion efficiency, η_p percent	Total pressure drop through combustor, ΔP in. Hg	Combustion parameter, $V_r/P_1 T_1$ ft, lb, sec, or units
Model 13B												
541	5.0	728	0.513	0.703	79.4	17.9	0.0098	1281	553	73.8	0.46	298x10 ⁶
542		722	.511	.700	78.5	19.5	.0105	1390	668	82.1	.47	297
543		722	.511	.700	78.5	22.5	.0122	1475	753	80.8	.45	297
544		728	.511	.700	79.1	27.4	.0149	1538	810	72.3	.43	297
Model 13C												
545	8.0	728	0.834	1.142	80.7	---	---	---	---	---	---	189x10 ⁶
546	5.0	727	.519	.711	80.4	---	---	---	---	---	---	501
547	5.0	721	.521	.714	79.9	16.1	0.0086	1270	549	82.0	0.44	302
548		726	.521	.714	80.5	18.7	.0100	1349	623	80.8	.46	302
549		728	.522	.715	80.8	22.9	.0122	1523	795	86.1	.51	303
550		724	.528	.723	81.4	21.3	.0112	1431	707	82.4	.50	306
551		724	.521	.714	80.2	27.9	.0148	1680	956	86.3	.52	302
552		729	.521	.714	80.8	34.3	.0183	1850	1121	83.8	.54	302
553		722	.521	.714	80.0	41.5	.0221	1934	1212	76.1	.55	302
554	8.0	726	.833	1.142	80.4	22.8	.0076	1310	584	98.4	.67	189
555		725	.836	1.146	80.3	28.4	.0094	1432	709	97.7	.72	189
556		724	.829	1.136	79.8	34.3	.0115	1548	824	94.5	.75	188
557	8.05	727	.838	1.148	80.6	41.6	.0137	1659	932	90.4	.78	187
558	8.0	723	.832	1.140	80.0	47.7	.0159	1789	1046	88.8	.79	188
559		726	.834	1.143	80.5	58.6	.0195	1966	1240	87.9	.84	189
Model 13D												
560	5.0	726	0.523	0.716	80.9	17.5	0.0092	1274	548	76.1	0.45	304x10 ⁶
561		726	.523	.717	81.0	20.8	.0110	1387	661	78.0	.46	304
562		729	.521	.714	81.0	25.1	.0133	1527	798	79.1	.49	303
563		727	.522	.715	80.8	27.9	.0148	1644	917	82.7	.51	303
564		728	.520	.713	80.7	30.8	.0164	1756	1028	84.7	.52	302
565		729	.522	.715	81.1	34.2	.0182	1859	1130	85.0	.53	303
566		727	.521	.714	80.8	38.1	.0203	1947	1220	83.2	.54	303
567	8.1	726	.838	1.149	79.9	22.7	.0075	1261	535	91.1	.66	185
568	8.0	728	.837	1.148	81.0	27.9	.0092	1417	689	96.8	.70	190
569		728	.832	1.141	80.6	35.5	.0118	1585	837	93.5	.73	189
570		728	.833	1.142	80.7	42.6	.0142	1705	977	92.4	.76	189
571		728	.831	1.140	80.5	50.5	.0188	1834	1106	88.3	.79	188
572		725	.830	1.138	80.1	60.5	.0202	1932	1287	87.0	.82	188
573	14.9	727	2.612	3.578	143.9	71.2	.0075	1233	566	96.0	---	170
574	15.0	726	2.628	3.601	143.7	82.8	.0087	1392	666	98.7	---	168
575	15.05	727	2.641	3.618	144.1	96.8	.0099	1487	760	99.8	---	169
576	15.0	726	2.647	3.628	144.8	114.3	.0119	1630	904	100.2	---	170
577		724	2.650	3.630	144.5	145.9	.0152	1788	1064	94.2	---	171
578	15.15	727	2.627	3.599	142.1	163.2	.0172	1907	1180	93.7	---	166
579	15.2	728	2.630	3.603	141.9	171.8	.0181	1958	1230	93.4	---	165
Model 13E												
580	15.0	725	2.631	3.604	---	64.8	0.0068	1230	505	94.3	---	169x10 ⁶
581		724	2.635	3.610	---	76.8	.0080	1340	616	98.1	---	170
582		726	2.623	3.593	---	85.3	.0080	1430	704	101.4	---	169
583		726	2.636	3.611	---	97.9	.0103	1500	774	98.3	---	170
584		728	2.622	3.592	---	122.2	.0128	1655	927	95.5	---	169
585		730	2.639	3.615	---	151.2	.0159	1800	1070	91.2	---	170
586		731	2.626	3.597	---	175.9	.0186	1925	1194	88.4	---	169
587	5.0	718	.522	.715	---	21.4	.0114	1400	682	78.1	---	303
588		729	.521	.714	---	25.1	.0133	1525	796	78.9	---	303
589		733	.522	.715	---	29.3	.0155	1650	917	78.2	---	303
590		733	.521	.714	---	33.1	.0176	1780	1047	80.8	---	303
591		727	.519	.711	---	37.6	.0201	1900	1173	80.5	---	301
592		730	.521	.714	---	41.7	.0222	1850	1120	89.9	---	303
593	8.0	731	.831	1.139	---	19.9	.0068	1170	439	83.9	---	188
594		728	.832	1.141	---	25.6	.0085	1305	577	87.2	---	189
595		732	.832	1.141	---	29.5	.0098	1400	668	88.4	---	189
596		731	.830	1.138	---	33.4	.0111	1490	759	89.3	---	188
597		729	.838	1.149	---	41.4	.0137	1645	916	89.3	---	190
598		728	.832	1.141	---	49.2	.0164	1795	1067	88.3	---	189
599		729	.829	1.137	---	57.0	.0191	1945	1216	87.9	---	188
600		728	.831	1.139	---	64.7	.0216	2075	1346	87.2	---	188

TABLE II. - EXPERIMENTAL RESULTS - Continued



Run	Combustor-inlet total pressure, P_1 in. Hg	Combustor-inlet total temperature, T_1 °R	Air flow rate, W_a lb/sec	Air flow rate per unit area, W_a/A_r lb/(sec) (sq ft)	Combustor reference velocity, V_r ft/sec	Fuel flow rate, W_f lb/hr	Fuel-air ratio, f	Mean combustor-outlet temperature, T_o °R	Mean temperature rise through combustor, ΔT °F	Combustion efficiency, η_b percent	Total pressure drop through combustor, ΔP in. Hg	Combustion parameter, $V_r/P_1 T_1$ ft, lb, sec, °R units
Model 13F												
601	5.0	724	0.521	0.713	80.4	17.4	0.0083	1308	584	81.2	---	---
602		730	.518	.709	80.6	21.7	.0116	1454	724	81.6	---	---
603		728	.521	.713	80.8	25.0	.0133	1538	810	80.5	---	---
604		724	.520	.712	80.2	28.8	.0154	1623	899	78.2	---	---
605		724	.520	.712	80.2	33.1	.0178	1698	974	74.7	---	---
606		723	.518	.709	79.8	41.7	.0223	1603	880	53.8	---	---
607	8.0	728	.845	1.158	81.8	20.9	.0068	1238	510	94.7	---	---
608		730	.845	1.155	81.9	27.0	.0091	1373	643	93.6	---	---
609	8.05	726	.843	1.155	81.0	31.2	.0102	1456	750	92.8	---	---
610	8.0	729	.841	1.153	81.6	35.1	.0115	1528	799	91.0	---	---
611		724	.842	1.154	81.2	43.1	.0142	1668	944	88.9	---	---
612		728	.840	1.152	81.4	51.5	.0170	1788	1080	84.8	---	---
613		724	.839	1.150	80.8	59.9	.0198	1893	1169	81.3	---	---
614		728	.837	1.147	81.0	73.2	.0242	1954	1266	70.8	---	---
615	15.0	726	2.640	3.616	144.5	65.4	.0068	1308	582	108.5	---	---
616	15.05	735	2.632	3.605	145.5	81.0	.0855	1440	705	107.3	---	---
617	15.0	726	2.643	3.621	144.6	105.6	.0111	1528	802	95.2	---	---
618		726	2.637	3.612	144.6	128.7	.0135	1638	911	89.7	---	---
619		727	2.630	3.603	144.3	163.4	.0172	1685	958	75.2	---	---
620		728	2.648	3.627	145.5	189.7	.0198	1648	920	63.0	---	---
Model 13G												
621	5.0	731	0.523	0.716	81.4	16.5	0.0088	1260	529	82.5	---	---
622		728	.527	.721	81.7	24.2	.0127	1415	687	70.8	---	---
623		724	.528	.720	81.1	34.0	.0179	1395	671	49.9	---	---
624		728	.523	.716	80.9	38.6	.0205	1445	719	47.3	---	---
625		724	.523	.716	80.6	46.7	.0248	1495	771	42.5	---	---
Model 13H												
626	5.0	731	0.525	0.719	81.7	18.0	0.0095	1313	582	84.3	---	---
627		725	.528	.723	81.6	21.5	.0113	1417	692	82.5	---	---
628		728	.522	.715	80.9	25.5	.0136	1547	819	80.0	---	---
629		729	.522	.715	81.0	28.1	.0149	1612	883	79.0	---	---
630		728	.522	.715	80.9	32.1	.0171	1750	1022	81.0	---	---
631		725	.525	.716	80.8	37.9	.0201	1802	1177	80.8	---	---
632		723	.521	.713	80.2	53.7	.0288	2044	1321	65.8	---	---
633	15.0	724	2.644	3.622	144.2	73.2	.0078	1315	591	98.9	---	---
634		724	2.638	3.614	143.9	82.2	.0088	1387	663	99.3	---	---
635		732	2.622	3.592	144.6	91.0	.0096	1465	733	99.4	---	---
636		734	2.647	3.626	146.4	108.8	.0114	1580	846	98.0	---	---
637		733	2.649	3.629	146.4	126.4	.0132	1700	987	97.7	---	---
638		730	2.637	3.612	145.1	134.4	.0141	1748	1018	96.7	---	---
639		732	2.648	3.627	146.2	149.4	.0156	1830	1098	95.2	---	---
640		730	2.644	3.622	145.6	155.5	.0163	1872	1142	95.3	---	---
641	8.0	729	.832	1.140	80.7	22.4	.0074	1250	521	91.6	---	---
642		728	.834	1.142	80.8	29.2	.0097	1412	684	91.5	---	---
643		733	.838	1.148	81.7	34.4	.0114	1505	772	89.2	---	---
644		729	.835	1.144	81.0	44.9	.0149	1710	981	88.3	---	---
645	7.95	726	.829	1.136	80.6	50.0	.0167	1810	1084	87.9	---	---
646	8.0	730	.835	1.144	81.1	55.5	.0184	1905	1175	87.5	---	---
647		732	.833	1.141	81.1	61.1	.0203	1998	1266	86.3	---	---
Model 13I												
648	5.0	734	0.522	0.715	81.6	14.6	0.0077	1280	548	80.2	---	---
649		724	.522	.715	80.6	18.0	.0096	1375	651	88.0	---	---
650		730	.520	.713	80.9	23.9	.0127	1545	815	84.7	---	---
651		729	.522	.715	81.1	27.5	.0146	1655	926	84.6	---	---
652		724	.517	.708	79.8	31.2	.0167	1765	1041	84.2	---	---
653		727	.520	.713	80.6	36.2	.0193	1915	1188	84.7	---	---
654		732	.521	.714	81.3	43.9	.0233	2070	1358	80.6	---	---
655	8.0	732	.827	1.133	80.5	22.1	.0074	1285	553	95.8	---	---
656		724	.827	1.133	79.6	26.9	.0090	1415	691	99.2	---	---
657		725	.826	1.135	79.9	32.6	.0109	1510	785	94.4	---	---
658		727	.830	1.137	80.2	39.3	.0131	1640	913	92.6	---	---
659		732	.830	1.137	80.8	49.6	.0166	1843	1111	91.3	---	---
660		726	.831	1.138	80.2	54.0	.0180	1930	1204	91.6	---	---
661		732	.827	1.133	80.5	63.5	.0213	2100	1368	89.8	---	---

TABLE II. - EXPERIMENTAL RESULTS - Continued



Run	Combustor-inlet total pressure, P_1 in. Hg	Combustor-inlet total temperature, T_1 or T_R	Air flow rate, W_a lb/sec	Air flow rate per unit area, W_a/A_p lb/(sec sq ft)	Combustor reference velocity, V_r ft/sec	Fuel flow rate, W_f lb/hr	Fuel-air ratio, f	Mean combustor-outlet temperature, T_0 or T_{0f}	Mean temperature rise through combustor, ΔT_{0f}	Combustion efficiency, η_b percent	Total pressure drop through combustor, ΔP in. Hg	Combustion parameter, $V_r/P_1 T_1$ ft, lb, sec, or units
Model 13J												
862	5.0	728	0.520	0.713	80.7	15.2	0.0081	1290	562	88.9	---	---
863		725	.520	.713	80.4	20.2	.0108	1430	705	84.7	---	---
864		729	.520	.713	80.8	24.6	.0131	1550	821	82.9	---	---
865		732	.520	.713	81.2	28.3	.0151	1660	928	82.5	---	---
866		732	.519	.711	80.9	32.1	.0172	1760	1028	81.2	---	---
867	15.0	726	.519	.711	80.4	38.7	.0207	1925	1199	80.3	---	---
868		724	.519	.711	80.1	48.4	.0259	2110	1366	76.0	---	---
869		723	2.631	3.604	143.4	51.0	.0053	1185	462	108.8	---	---
870		720	2.638	3.614	143.1	64.2	.0067	1290	570	108.1	---	---
871		727	2.638	3.614	144.6	81.6	.0085	1415	688	104.0	---	---
872	15.2	727	2.638	3.614	144.6	104.2	.0109	1560	833	100.2	---	---
873		722	2.624	3.595	142.8	121.7	.0128	1710	988	102.6	---	---
874		725	2.638	3.614	144.2	146.3	.0154	1835	1110	97.86	---	---
875		726	2.637	3.612	142.3	169.0	.0178	1980	1264	87.11	---	---
Model 13I												
876	15.0	722	2.629	3.601	143.0	59.8	0.0083	1190	468	94.6	---	---
877		727	2.644	3.622	145.1	83.0	.0087	1405	678	101.0	---	---
878		728	2.640	3.616	145.0	93.5	.0098	1480	752	100.0	---	---
879		728	2.641	3.618	145.0	108.6	.0114	1595	862	99.9	---	---
880		724	2.625	3.598	143.2	123.9	.0131	1705	981	100.2	---	---
881	15.2	725	2.633	3.607	143.9	137.0	.0144	1790	1065	99.5	---	---
882		725	2.640	3.616	144.3	152.3	.0160	1890	1165	99.2	---	---
883		726	2.617	3.585	140.8	181.8	.0193	2050	1334	96.1	---	---
884		726	2.623	3.593	138.8	210.7	.0223	2170	1444	91.3	---	---
885		724	2.635	3.610	143.7	241.3	.0264	2250	1526	104.0	---	---
886	15.0	731	1.558	2.134	80.6	30.2	.0053	1185	434	102.1	---	---
887		733	1.567	2.147	81.3	37.9	.0067	1270	537	102.3	---	---
888		733	1.564	2.142	81.2	51.1	.0090	1442	709	101.8	---	---
889		733	1.565	2.144	81.2	59.4	.0105	1550	817	102.1	---	---
890		731	1.562	2.140	80.8	67.3	.0119	1650	919	102.1	---	---
891	15.0	733	1.563	2.141	81.1	82.8	.0147	1832	1099	101.0	---	---
892		733	1.560	2.137	80.9	90.0	.0160	1920	1187	101.2	---	---
893		728	1.558	2.134	80.3	124.0	.0221	2225	1497	95.7	---	---
Model 13J												
894	8.0	733	0.832	1.141	81.2	21.7	0.0072	1280	527	93.4	---	---
895		733	.829	1.137	80.9	29.1	.0097	1410	677	90.5	---	---
896		733	.830	1.138	81.0	36.7	.0122	1565	832	89.7	---	---
897		727	.828	1.137	80.2	42.4	.0142	1690	963	90.9	---	---
898		730	.830	1.138	80.6	48.1	.0161	1800	1070	90.3	---	---
899	8.0	729	.831	1.140	80.6	55.6	.0185	1930	1201	89.1	---	---
900		728	.830	1.137	80.3	73.6	.0246	2195	1467	84.7	---	---
Model 15I												
701	5.0	732	0.523	0.717	81.7	---	---	---	---	---	0.21	---
702	8.0	735	.832	1.140	81.3	---	---	---	---	---	.31	---
703	5.0	724	.522	.715	80.6	16.2	0.0086	1270	546	81.2	.28	323x10 ⁶
704		726	.521	.713	80.6	24.0	.0128	1420	694	71.2	.50	322
705		721	.520	.713	80.0	35.7	.0190	1545	824	43.7	.29	322
706		723	.520	.713	80.2	19.3	.0103	1320	597	83.7	.31	322
707		728	.520	.713	80.7	23.9	.0128	1450	722	82.0	.31	322
708	5.0	729	.521	.714	81.0	28.9	.0154	1570	841	78.9	.32	322
709		726	.522	.715	80.7	36.1	.0182	1645	919	73.5	.34	323
710		728	.520	.713	80.7	45.2	.0241	1900	1172	76.5	.38	322
Model 13J												
711	5.0	722	0.522	0.715	80.4	14.6	0.0078	1245	525	86.1	---	---
712		732	.522	.715	81.5	21.5	.014	1435	703	80.7	---	---
713		728	.523	.716	81.1	25.2	.0133	1550	822	81.8	---	---
714		732	.523	.716	81.5	28.5	.0151	1655	923	81.8	---	---
715		728	.522	.715	81.0	32.0	.0170	1755	1027	81.9	---	---
716	5.0	724	.522	.715	80.6	39.5	.0210	1930	1206	79.7	---	---
717		728	.522	.715	81.0	39.4	.0209	1960	1232	89.3	---	---
718		728	.522	.715	81.0	61.9	.0329	2105	1377	80.6	---	---
719		728	.522	.715	81.0	61.9	.0329	2220	1492	71.5	---	---
720		728	.522	.715	81.0	18.7	.0089	1320	592	86.0	---	---
721	5.0	722	.522	.715	80.4	18.7	.0089	1315	593	86.3	---	---
Model 13A												
722	5.0	730	0.520	0.712	80.8	17.3	0.0092	1295	565	78.7	0.49	321x10 ⁶
723		730	.519	.711	80.7	21.0	.0112	1420	690	80.2	.51	321
724		729	.519	.711	80.6	26.5	.0142	1580	851	79.9	.52	321
725		728	.518	.709	80.3	28.8	.0154	1655	927	80.6	.53	320
726		723	.521	.714	80.3	32.3	.0172	1760	1037	81.7	.55	322
727	5.0	726	.521	.714	80.6	38.8	.0206	1925	1199	80.4	.55	322

*Plus addition primary air.

TABLE II. - EXPERIMENTAL RESULTS - Concluded



Run	Combustor-inlet total pressure, P_1 in. Hg	Combustor-inlet total temperature, T_1 °R	Air flow rate, W_a lb/sec	Air flow rate per unit area, W_a/A_r lb/(sec sq ft)	Combustor reference velocity, V_r ft/sec	Fuel flow rate, W_f lb/hr	Fuel-air ratio, f	Mean combustor-outlet temperature, T_0 °R	Mean temperature rise through combustor, ΔT °F	Combustion efficiency, η_b percent	Total pressure drop through combustor, ΔP in. Hg	Combustion parameter, $V_r/P_1 T_1$ ft, lb, sec, °R units
Model 13A - Concluded												
728	5.0	728	0.520	0.712	80.7	18.8	0.0100	1340	812	79.0	0.50	521x10 ⁶
729		728	.520	.712	80.7	21.4	.0114	1435	707	80.9	.51	321
730		729	.521	.713	80.8	25.6	.0136	1580	831	80.8	.53	322
731		725	.519	.711	80.2	28.6	.0153	1655	930	81.5	.53	321
732		726	.519	.711	80.3	35.0	.0187	1830	1104	80.7	.55	321
733		728	.519	.711	80.5	46.7	.0250	1910	---	---	---	321
734	8.0	727	.830	1.137	80.2	22.4	.0075	1290	563	96.2	.70	200
735		729	.828	1.135	80.3	27.7	.0092	1385	656	91.7	.73	199
736		727	.827	1.133	79.8	37.2	.0125	1580	853	90.4	.77	199
737		724	.828	1.135	79.7	42.8	.0143	1705	981	91.7	.78	199
738		725	.828	1.135	79.8	48.6	.0163	1810	1085	90.4	.81	199
739		725	.828	1.135	79.8	60.1	.0201	2015	1290	88.9	.82	199
740	31.6	726	2.143	2.936	51.4	53.7	.0089	1510	584	107.6	---	---
741	31.6	720	2.053	2.812	48.8	68.2	.0092	1485	765	108.1	---	---
742	31.8	719	2.023	2.771	47.7	102.2	.0140	1835	1116	107.5	---	---
743	45.7	718	2.715	3.719	44.4	66.0	.0087	1500	582	110.4	---	---
744	46.0	728	2.627	3.599	45.2	101.5	.0107	1640	912	112.5	---	---
745	46.7	732	2.620	3.589	42.7	114.7	.0121	1770	1038	114.4	---	---
746	46.8	732	2.624	3.595	42.7	112.9	.0119	1730	998	111.6	---	---
Model 14T												
747	5.0	728	0.522	0.715	81.0	16.5	0.0087	1325	597	88.1	---	---
748		729	.518	.709	80.4	19.2	.0105	1400	671	84.7	---	---
749		730	.517	.708	80.4	21.3	.0113	1510	780	91.0	---	---
750		726	.514	.705	79.8	25.1	.0135	1630	904	89.0	---	---
751		728	.518	.709	80.1	28.3	.0152	1730	1004	88.1	---	---
752		723	.522	.715	80.4	32.2	.0171	1840	1117	88.9	---	---
753		730	.521	.715	81.0	34.8	.0185	1915	1185	87.8	---	---
754		729	.522	.715	81.1	52.7	.0280	2130	1401	71.6	---	---
755		724	.519	.711	80.1	17.5	.0093	1320	598	93.7	---	---
756		727	.519	.711	80.4	20.2	.0108	1440	713	95.4	---	---
757		728	.521	.714	80.9	23.7	.0126	1540	812	92.3	---	---
758		726	.519	.711	80.3	27.7	.0148	1685	959	96.2	---	---
759		729	.520	.712	80.7	34.1	.0182	1880	1151	94.0	---	---
Model 14K												
760	5.0	724	0.520	0.713	80.3	16.6	0.0088	1335	611	89.3	---	---
761		732	.519	.711	81.0	20.8	.0111	1450	718	84.5	---	---
762		724	.521	.714	80.4	28.0	.0149	1675	951	85.5	---	---
763		724	.517	.709	79.8	38.0	.0204	1915	1191	80.7	---	---
Model 14T												
764	15.0	720	2.850	3.630	143.8	58.0	0.0060	1160	440	91.8	---	---
765		720	2.852	3.633	143.9	72.1	.0075	1320	600	102.2	---	---
766		720	2.858	3.641	144.3	86.2	.0090	1440	720	104.0	---	---
767		725	2.825	3.596	143.3	98.7	.0104	1570	845	106.6	---	---
768		725	2.851	3.631	145.0	98.9	.0103	1560	835	106.0	---	---
769		725	2.851	3.631	145.0	115.6	.0121	1695	970	106.8	---	---
770		725	2.851	3.631	145.0	128.9	.0135	1780	1055	105.1	---	---
771		726	2.831	3.604	143.8	145.8	.0153	1905	1179	104.5	---	---
772		725	2.838	3.614	144.0	163.6	.0172	2036	1310	105.0	---	---
773		719	2.850	3.630	143.6	64.2	.0067	1255	516	97.8	---	---
774		725	2.644	3.622	144.5	78.3	.0082	1390	665	104.6	---	---
775		725	2.652	3.633	144.9	108.0	.0113	1630	905	106.1	---	---
776	5.0	729	.523	.716	81.2	18.7	.0099	1350	621	80.9	---	---
777		731	.522	.715	81.4	24.6	.0131	1590	859	87.2	---	---
778		731	.517	.709	80.6	31.0	.0168	1800	1089	87.4	---	---
779	15.0	726	2.641	3.618	144.5	78.1	.0082	1370	644	101.4	---	---
780	8.0	728	.830	1.137	80.3	19.8	.0068	1180	452	86.6	---	---
781		731	.828	1.132	80.2	24.7	.0083	1325	594	92.3	---	---
782		724	.832	1.140	80.1	27.9	.0093	1400	676	94.4	---	---
783		730	.832	1.141	80.8	34.0	.0113	1550	820	95.4	---	---
784		724	.831	1.139	80.0	41.3	.0138	1705	981	95.3	---	---
785		724	.833	1.142	80.2	51.6	.0172	1920	1195	92.0	---	---
786		730	.831	1.139	80.7	63.4	.0212	2120	1390	107.0	---	---
787	15.0	726	1.582	2.140	80.3	57.2	.0068	1280	554	107.3	---	---
788		729	1.550	2.123	80.0	48.1	.0068	1440	771	107.5	---	---
789		725	1.556	2.132	79.8	56.5	.0100	1550	825	107.5	---	---
790		724	1.550	2.125	78.4	64.0	.0114	1645	921	106.5	---	---
791		728	1.555	2.150	80.1	76.7	.0137	1905	1077	106.0	---	---
792		728	1.551	2.125	79.9	89.0	.0189	1950	1222	104.9	---	---
793		730	1.550	2.123	80.1	104.5	.0187	2105	1375	102.2	---	---

*Plus additional primary air.

bOutlet pressure rakes installed.

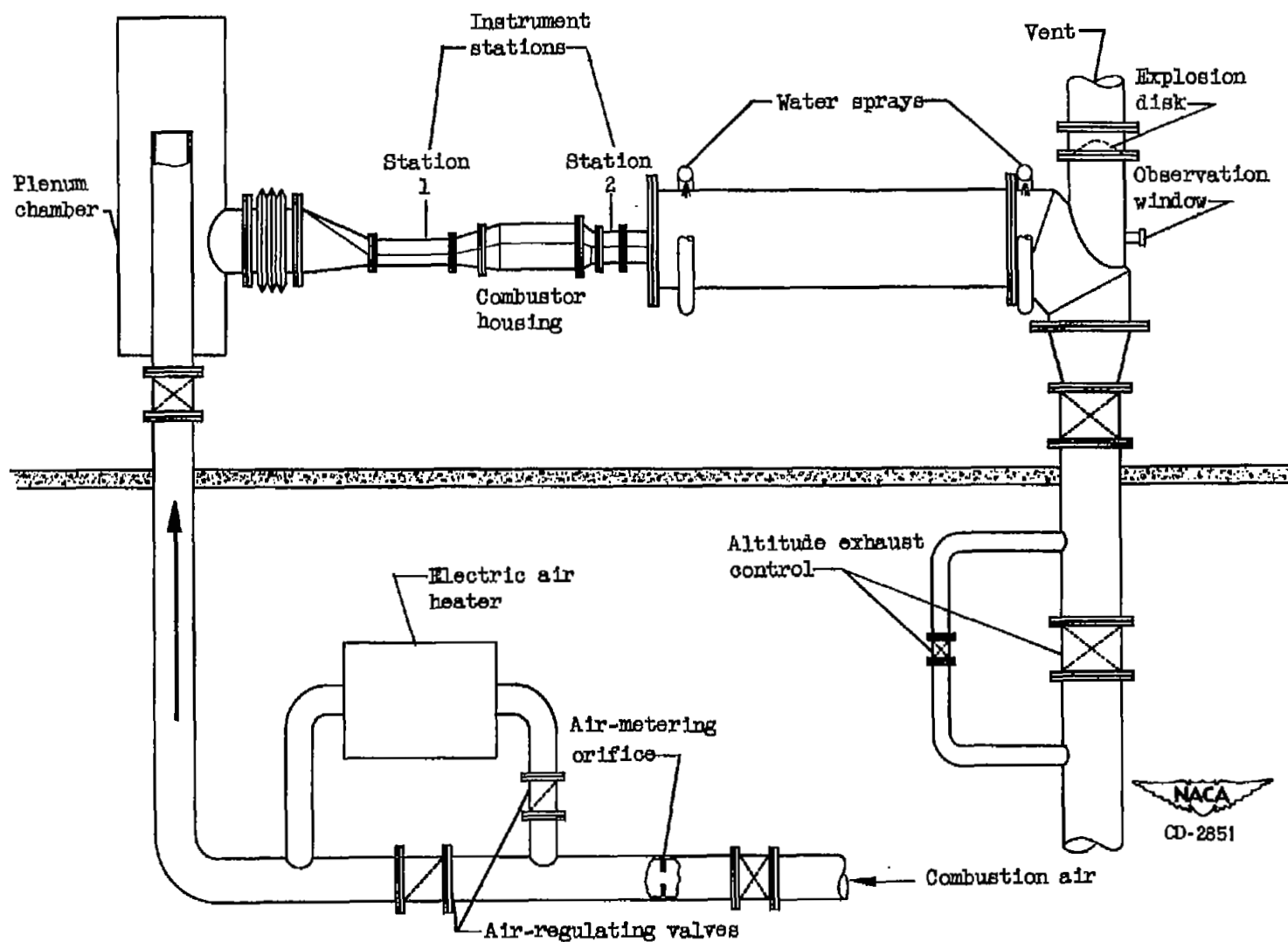
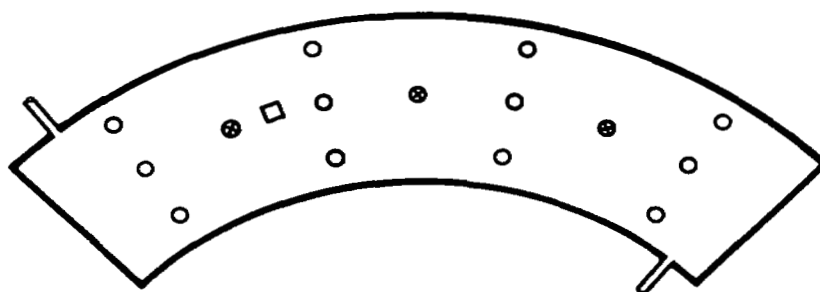
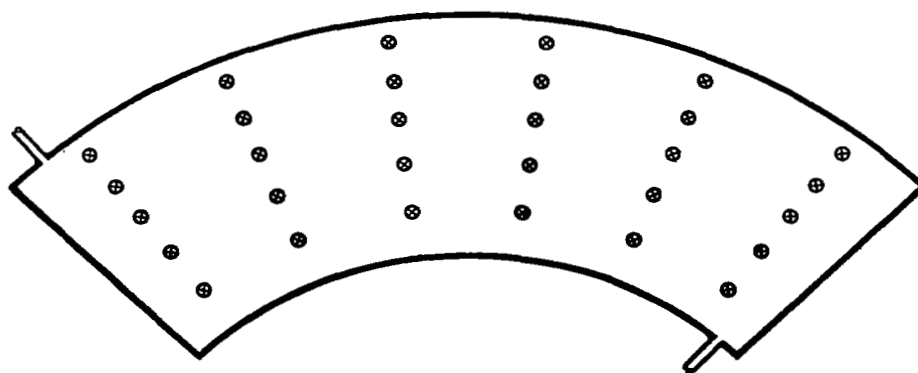


Figure 1. - Installation of one-quarter sector of 25 $\frac{1}{2}$ -inch-diameter annular combustor.



- ⊗ Thermocouple
- Total-pressure rake
- └┐ Static-pressure orifice
- Stream-static probe

(a) Inlet thermocouple (iron constantan), inlet total-pressure rakes, and stream static probe in plane at section 1.



NACA
CD-2845

(b) Outlet thermocouples (chromel-alumel) in plane at station 2.

Figure 2. - Locations of instrumentation.

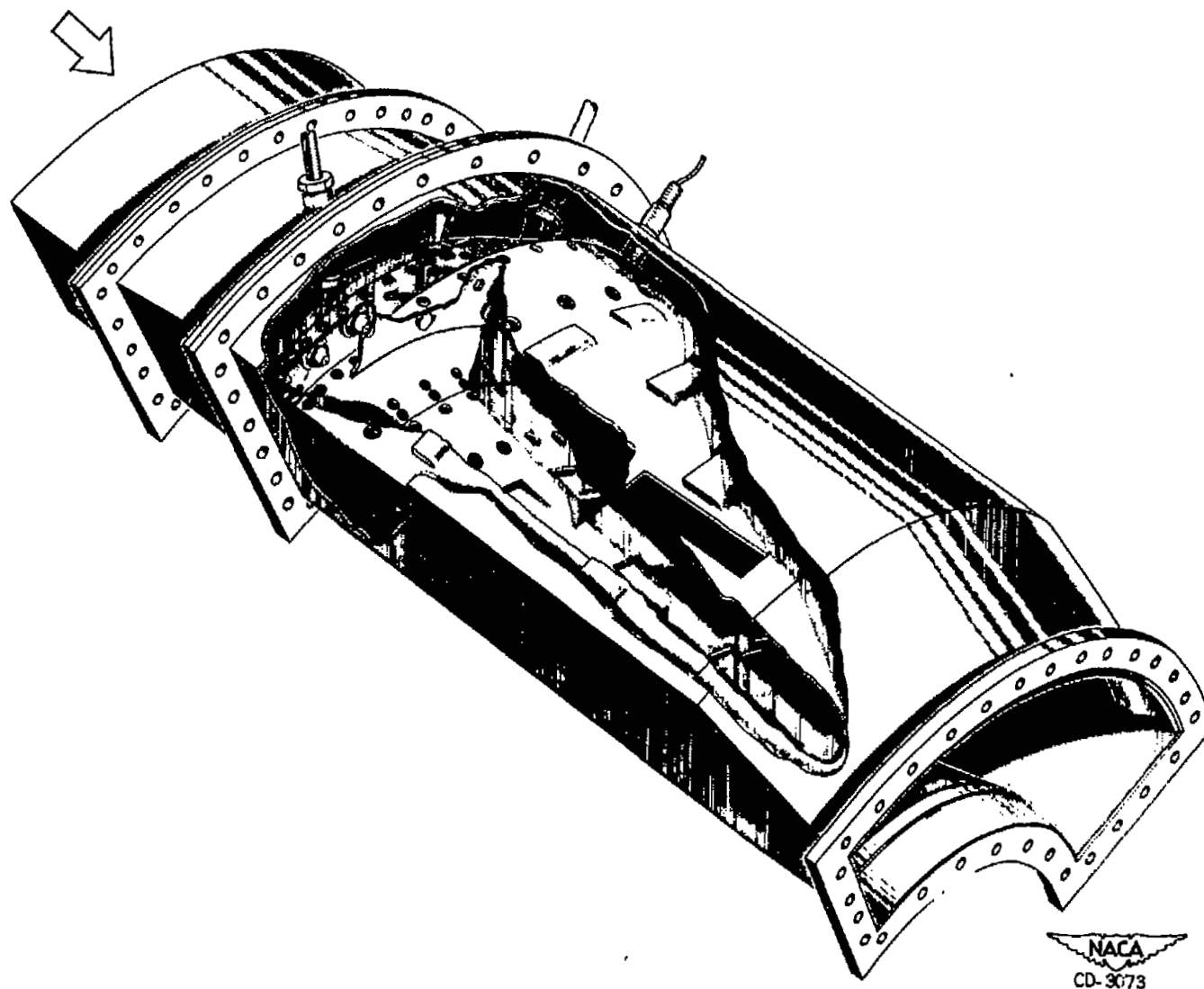


Figure 3. - One-quarter sector of model 13 annular combustor assembled in test ducting.

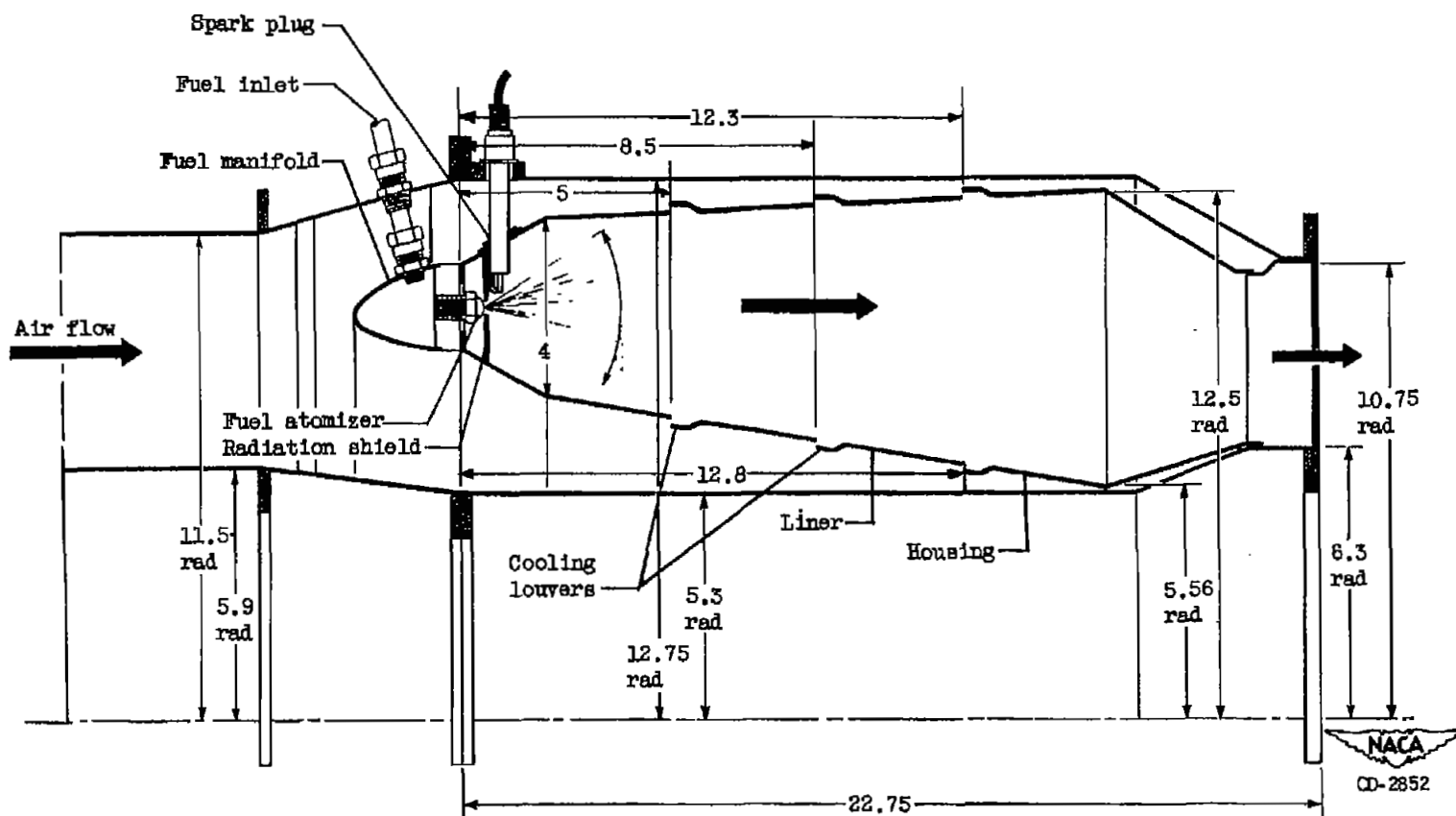


Figure 4. - Longitudinal cross-sectional view of model 13 combustor and housing. (Dimensions are in inches.)

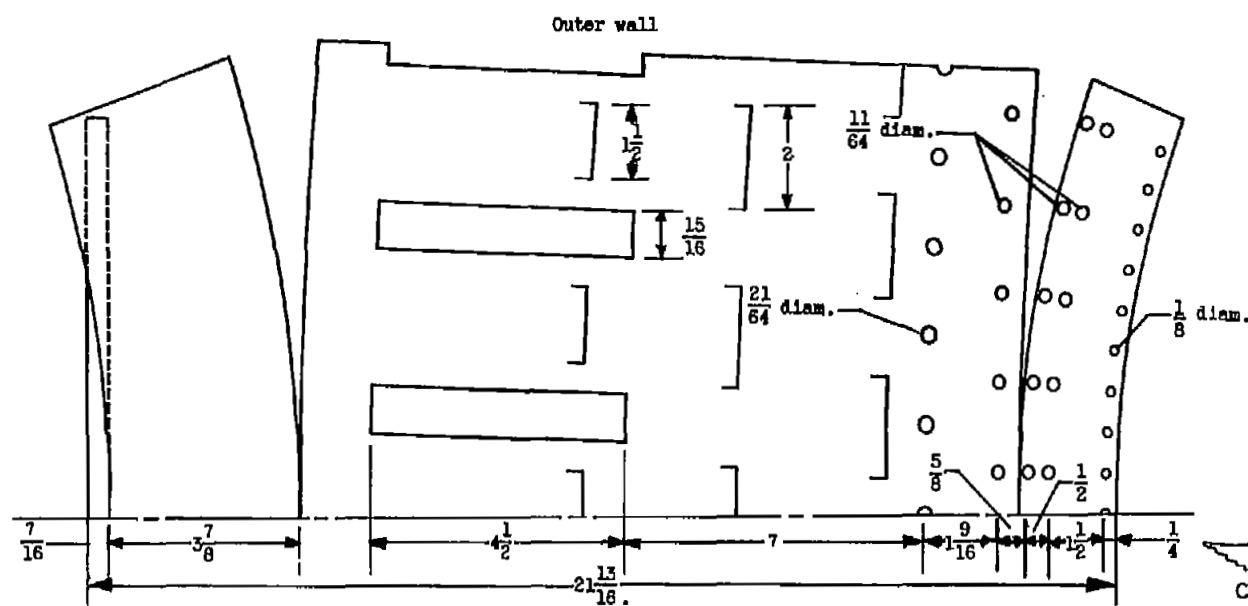
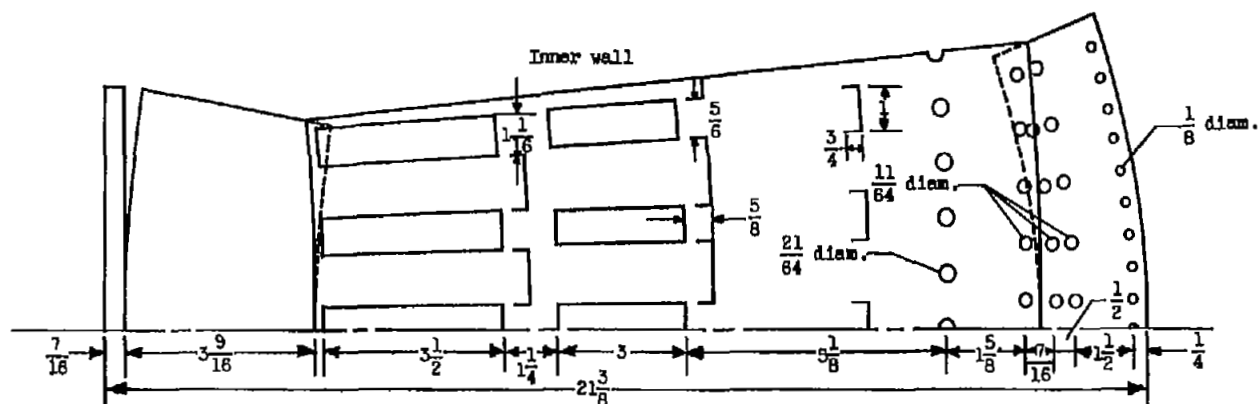


Figure 5. - Liner air-entry holes of model 13 combustor. (Dimensions are in inches.)

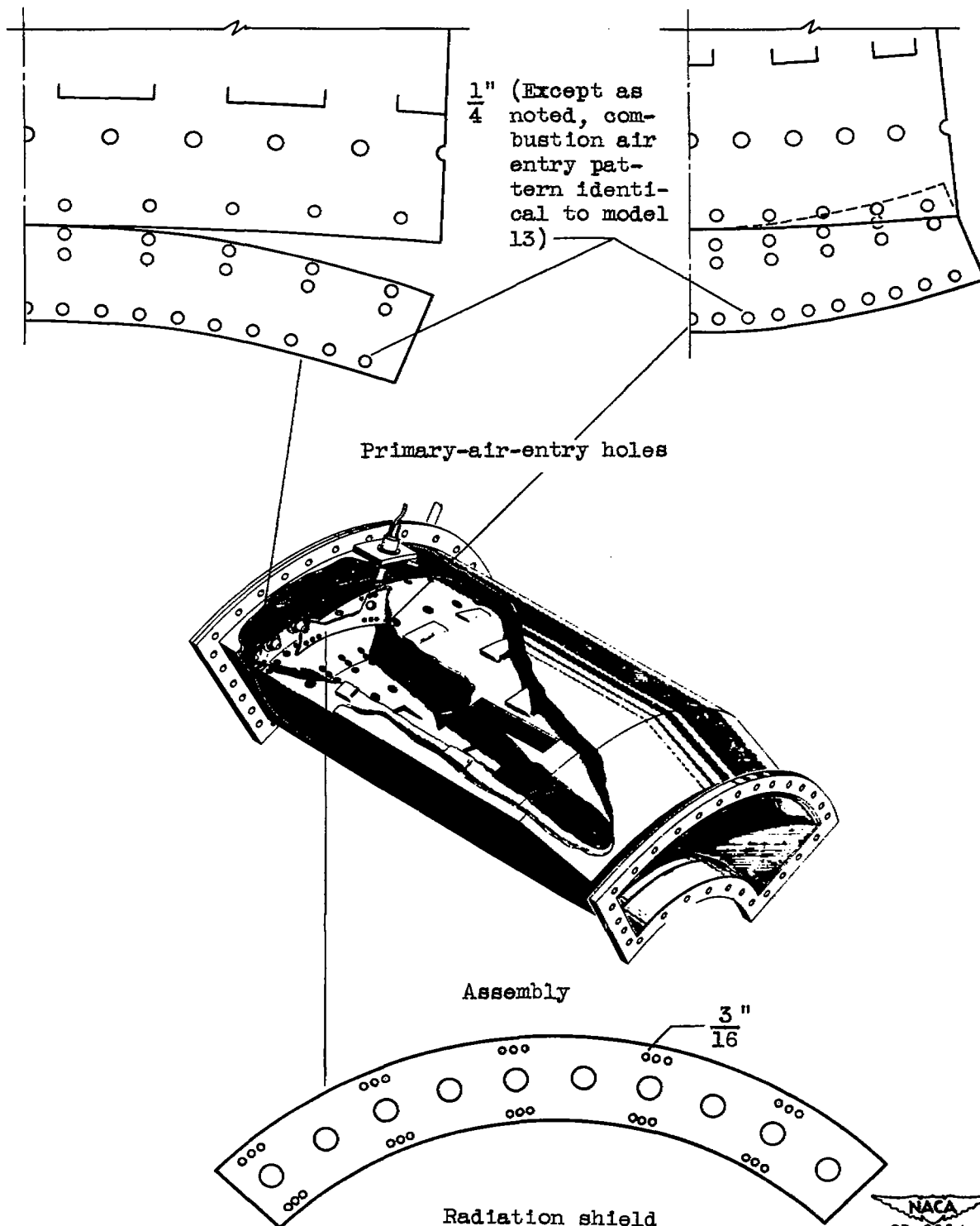


Figure 6. - One-quarter sector of model 14 annular combustor showing air entry and radiation shield modification.

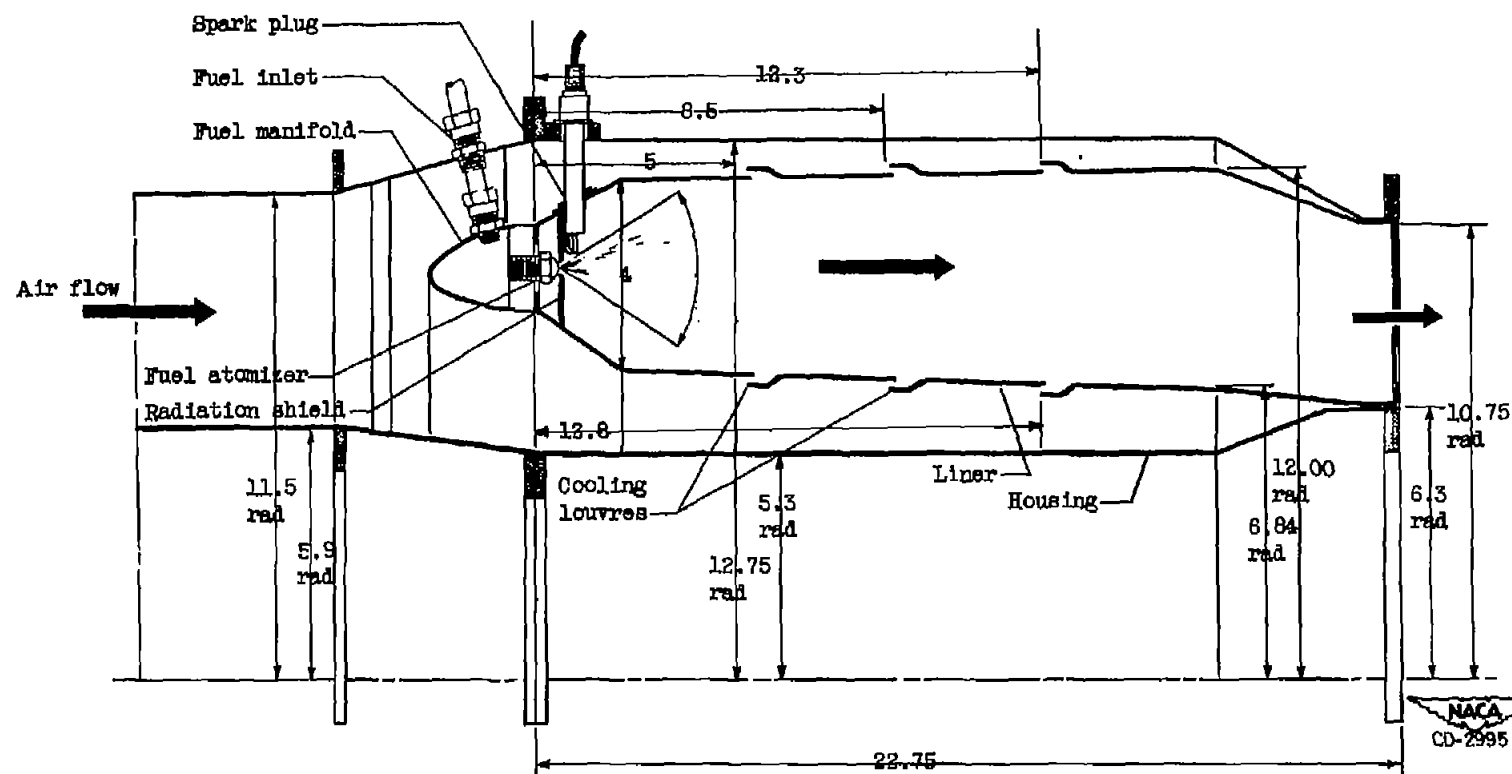


Figure 7. - Longitudinal cross-sectional view of model 15 combustor and housing. (Dimensions are in inches.)

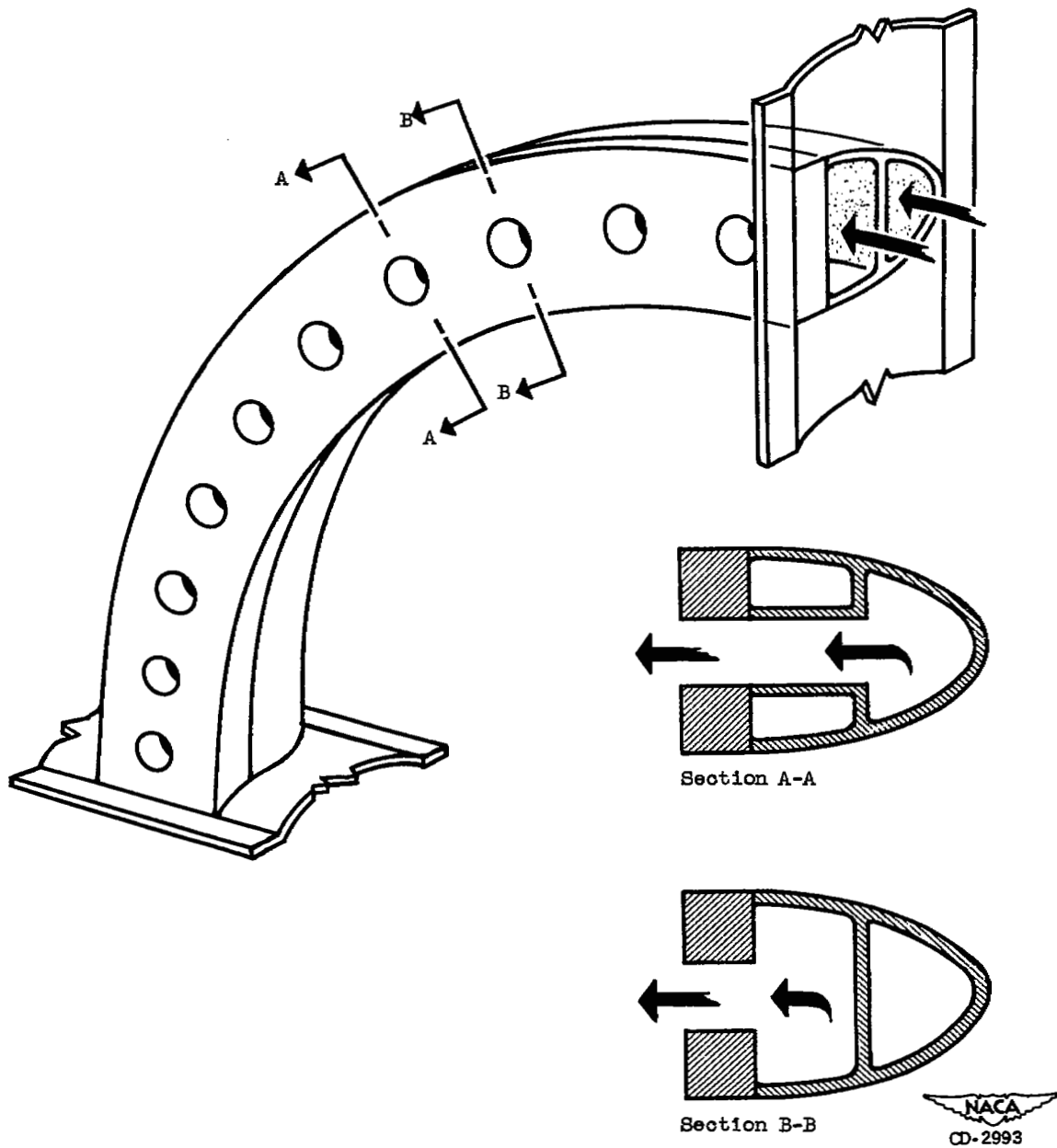
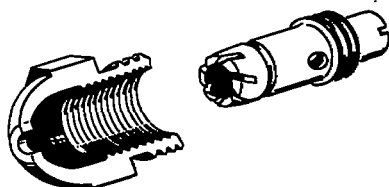
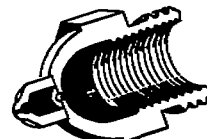


Figure 8. - Dual fuel manifold for one-quarter sector combustor.

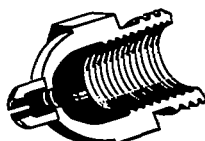
2837



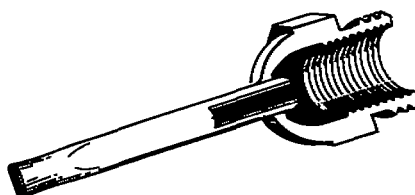
(a) Standard injector.



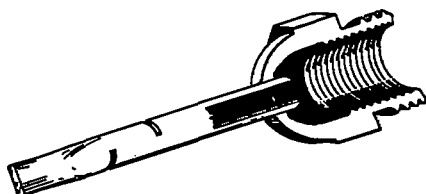
(b) Axial fan injector.



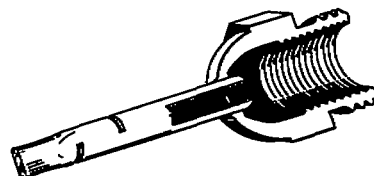
(c) Enlarged axial fan injector.



(d) Extended axial fan injector.



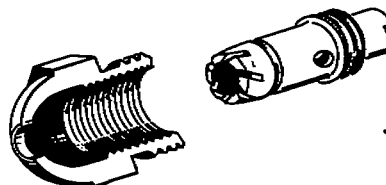
(e) Radial fan injector.



(f) Shorter radial fan injector.



(g) Sharp-edge orifice injector.



(h) Sharp-edge orifice injector with swirl.

NACA
CD-2992

Figure 9. - Cross-sectional view of fuel injectors.

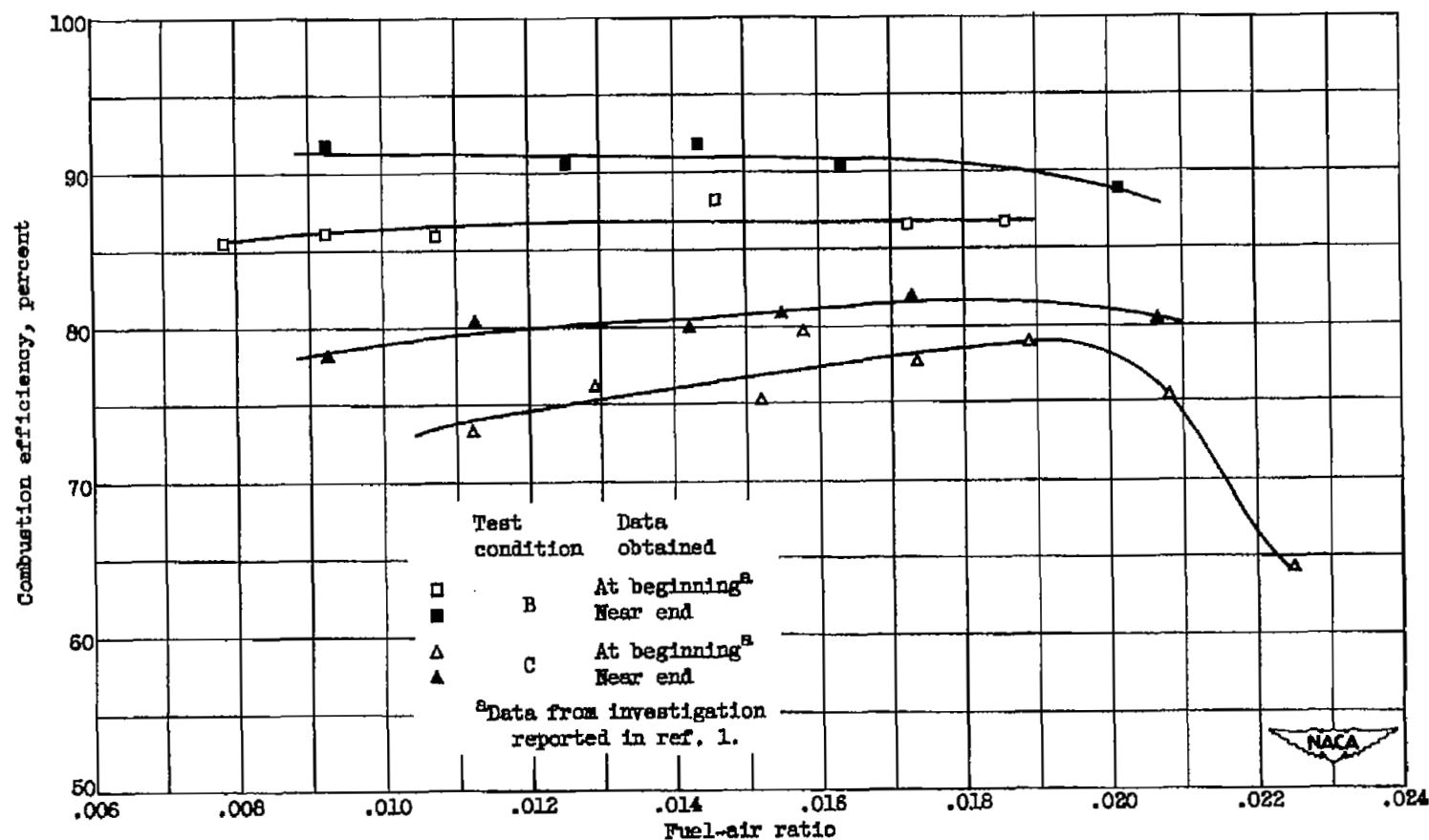


Figure 10. - Reproducibility of combustion efficiency data with combustor 13A. Comparison of data recorded prior to beginning and near conclusion of investigation reported herein. Fuel injectors: 30-gallon-per-hour, 70° swirl-type atomizers.

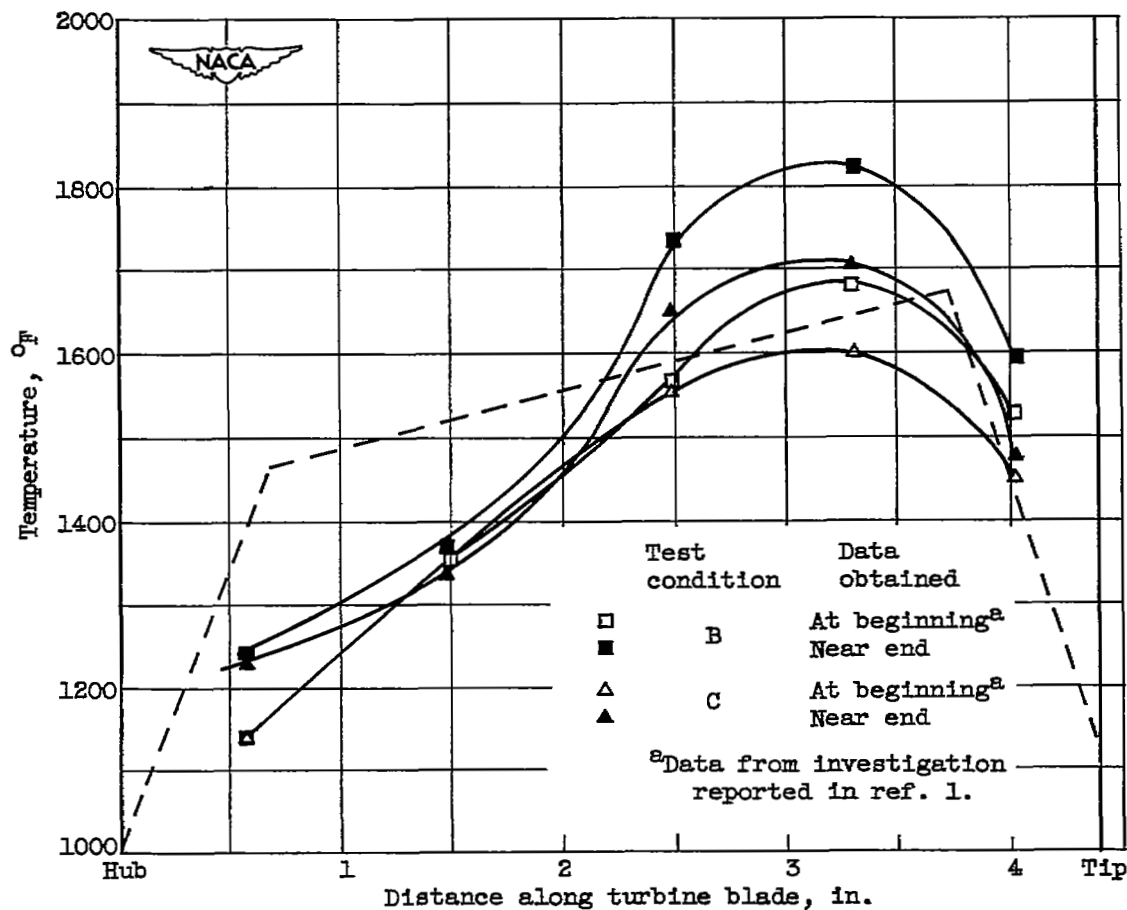


Figure 11. - Reproducibility of combustor-outlet temperature profile with combustor 13A. Comparison of data recorded at beginning and near conclusion of investigation reported herein. Fuel injectors: 30-gallon-per-hour, 70° swirl-type atomizers.

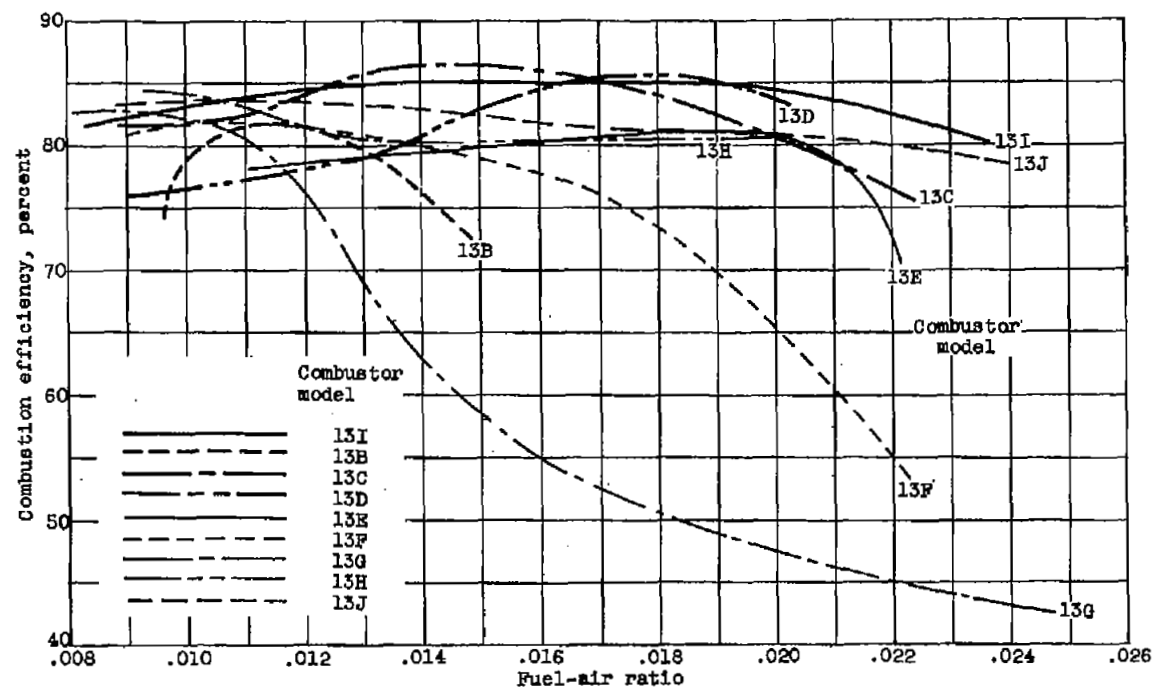


Figure 12. - Combustion efficiencies of model 13 combustor with various fuel injectors at test condition C. Comparison of data from appendix.

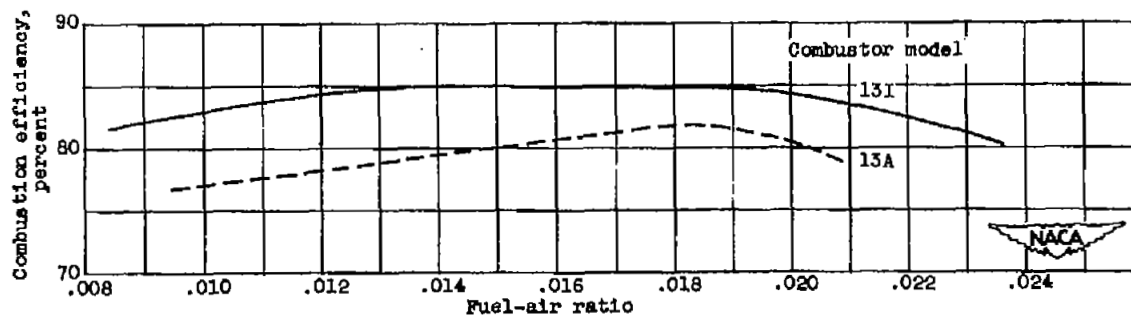


Figure 13. - Comparison of efficiency of model 13I combustor with that of model 13A at test condition C.

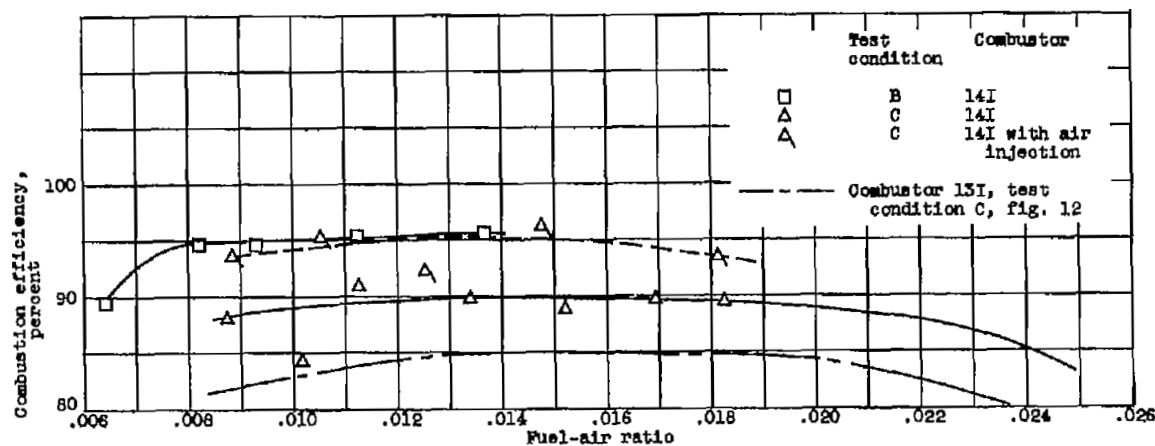


Figure 14. - Combustion efficiency of model 14I combustor at low pressures.

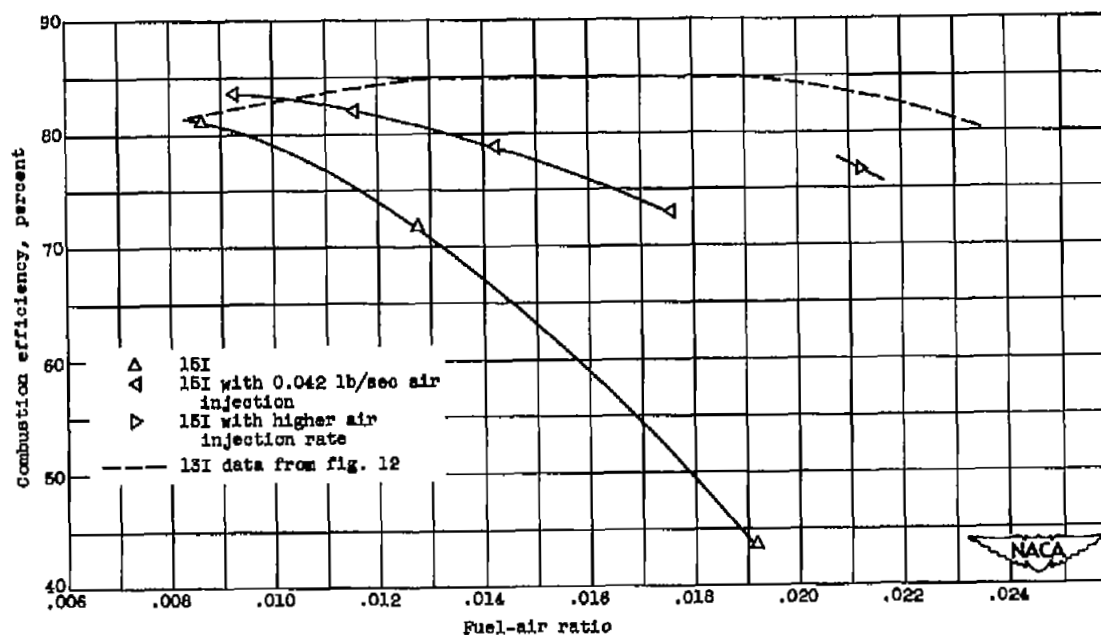


Figure 15. - Combustion efficiency of model 15I combustor at test condition C.

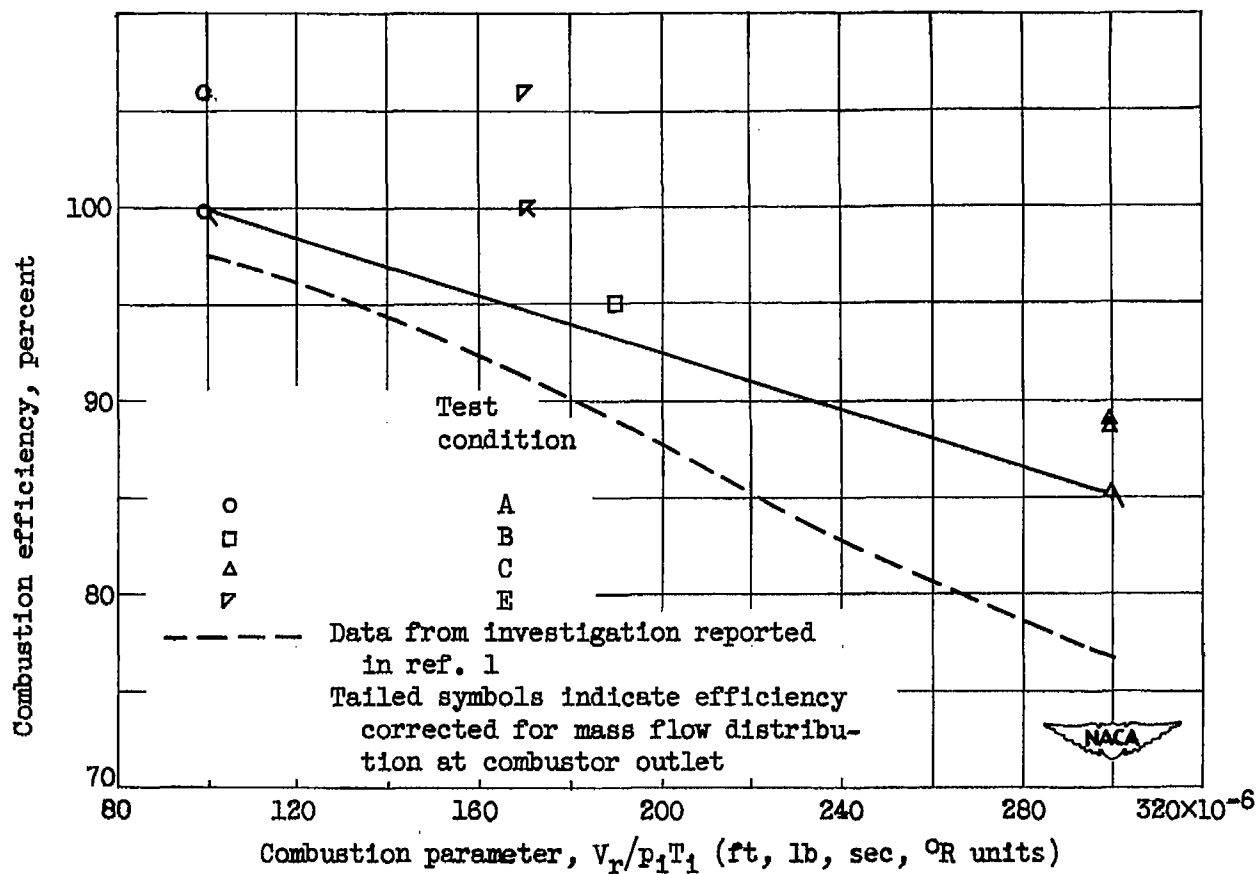


Figure 16. - Correlation of combustion efficiency data of model 14I combustor with combustion parameter $V_r/p_1 T_1$. Combustor temperature rise, 680° F.

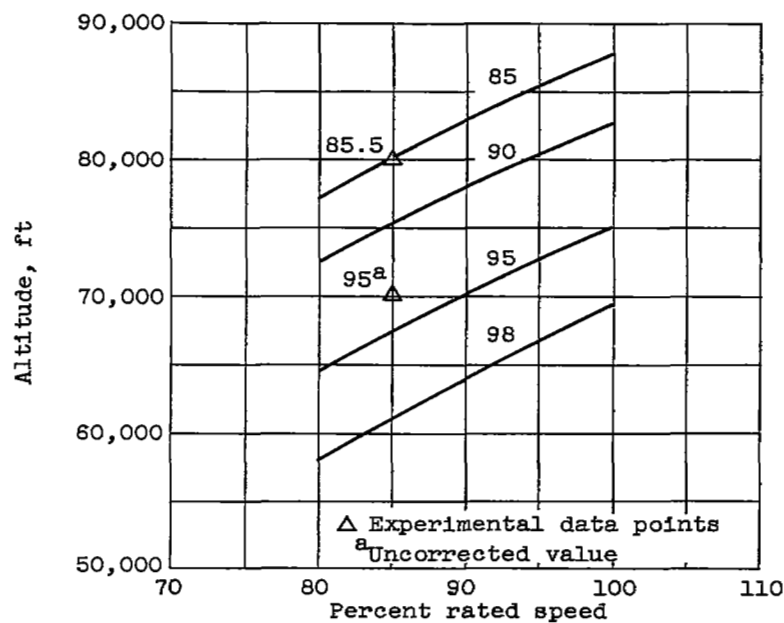


Figure 17. - Estimated altitude flight performance of model 14I combustor in 5.2 pressure ratio engine at flight Mach number 0.6. Efficiencies corrected for mass-flow distribution except for single value noted.

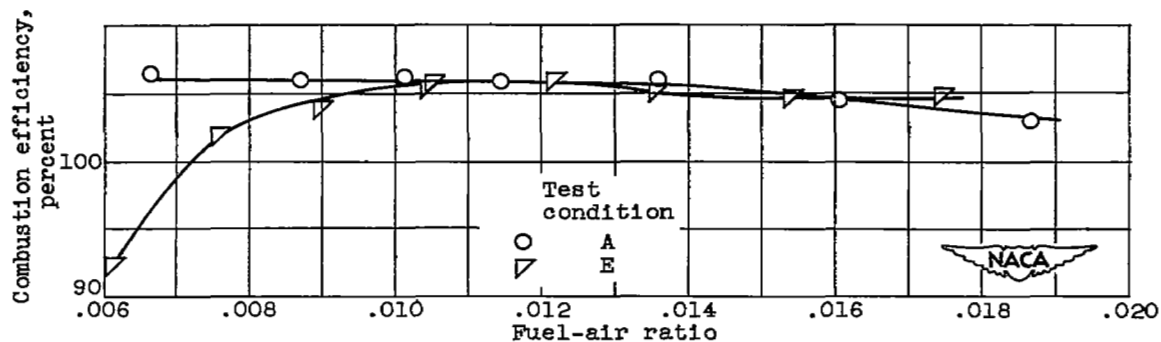
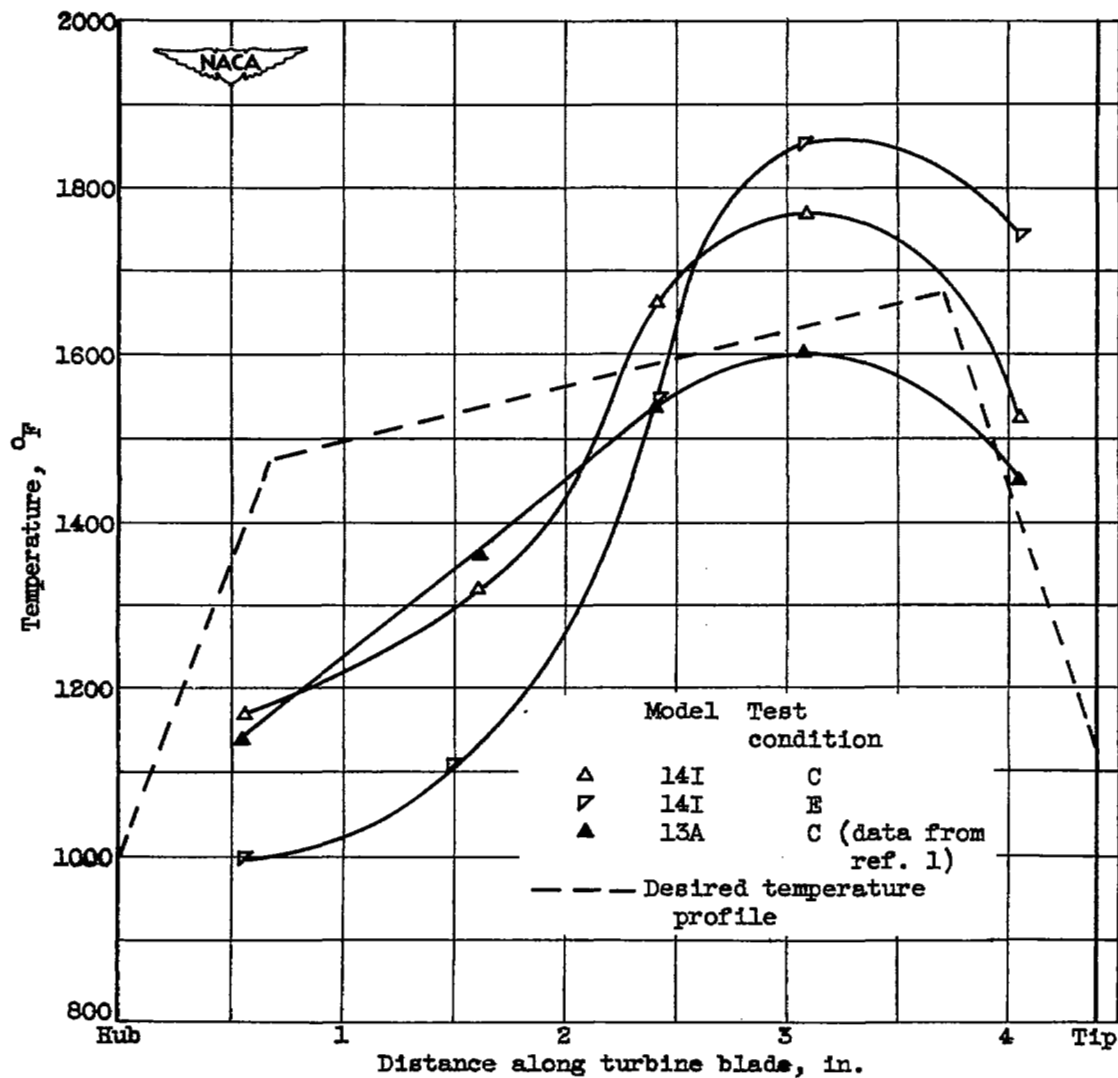
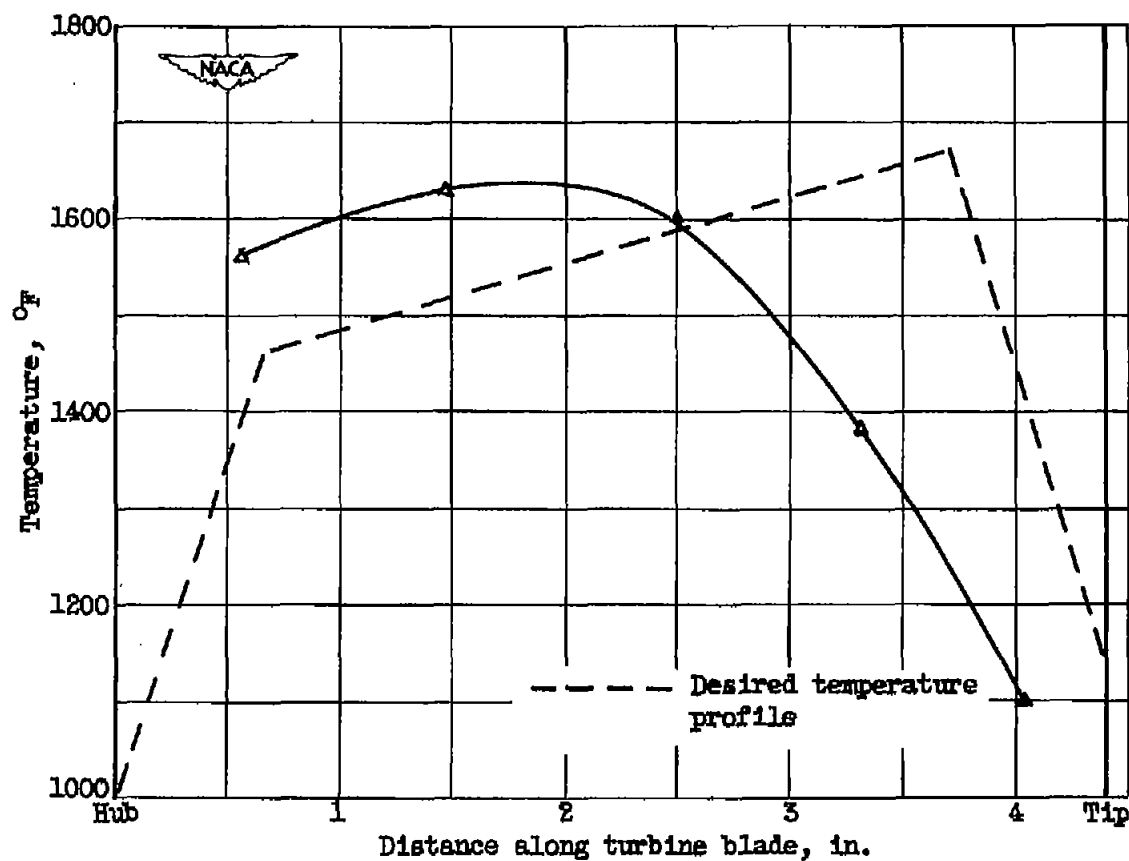


Figure 18. - Combustion efficiency of model 14I combustor at two air flow rates.



(a) Models 14I and 13A.

Figure 19. - Combustor-outlet radial temperature profiles.



(b) Model 15I.

Figure 19. - Concluded. Combustor-outlet radial temperature profiles.

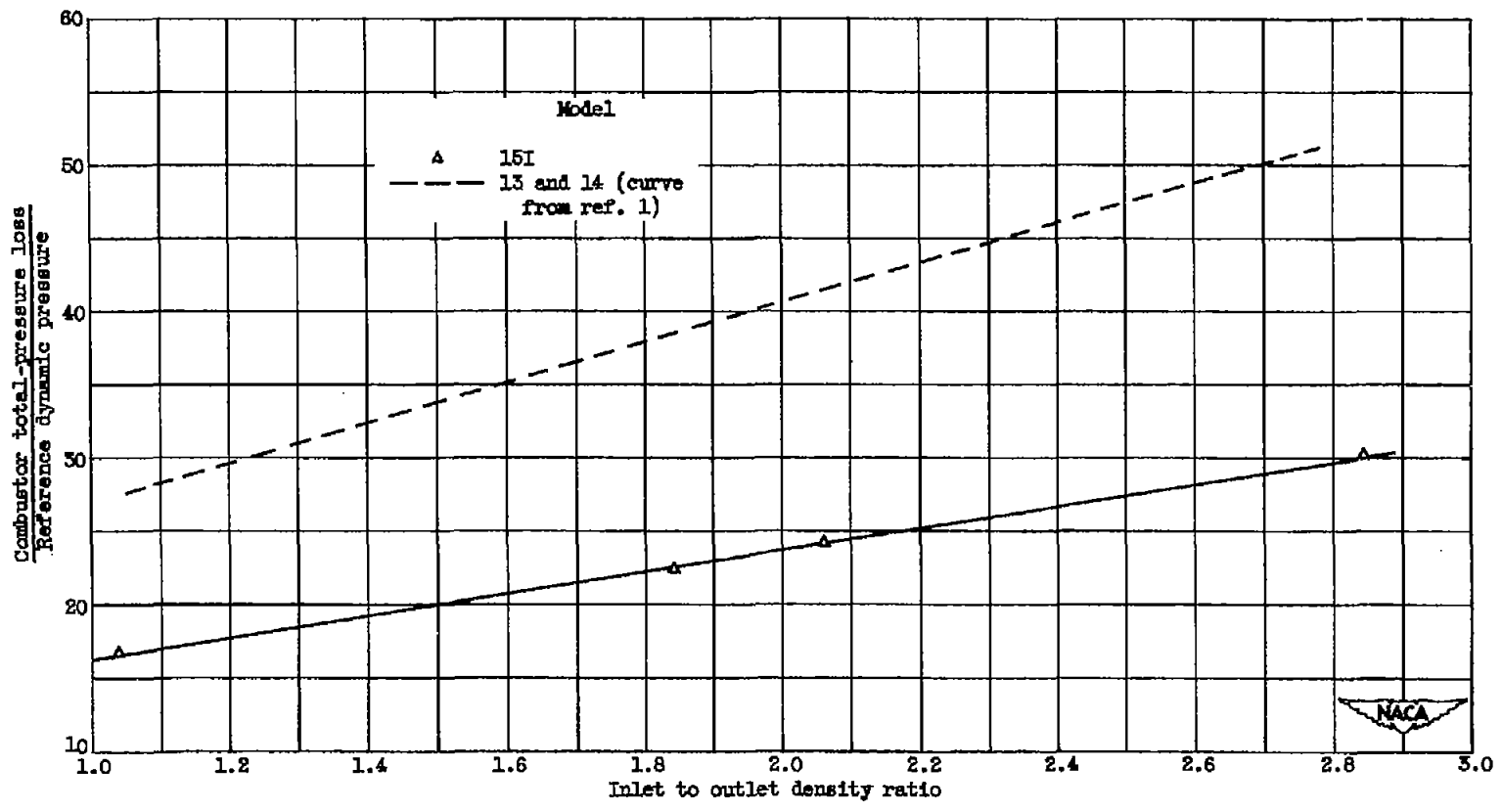
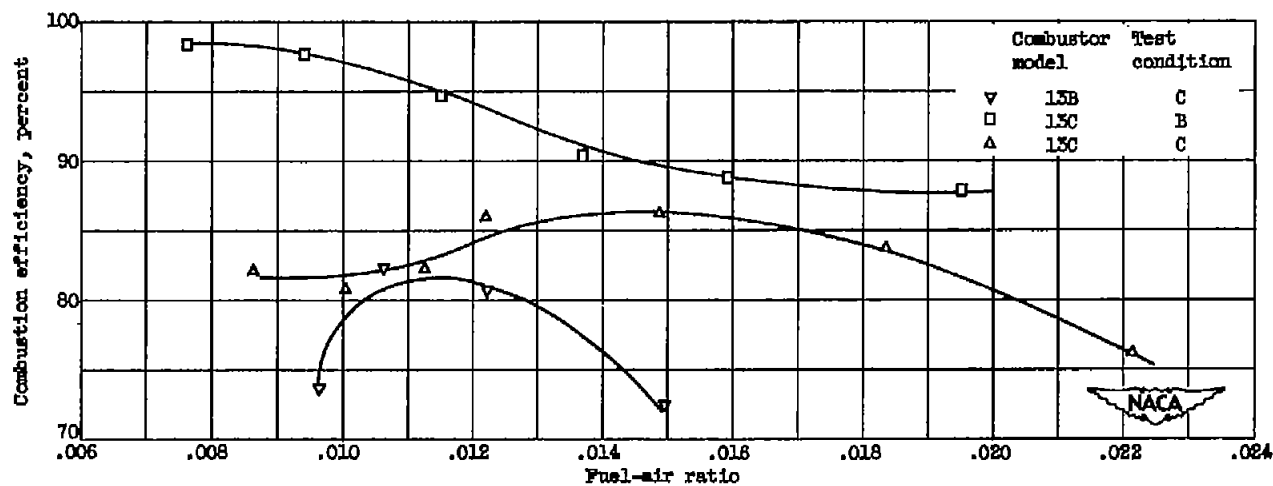
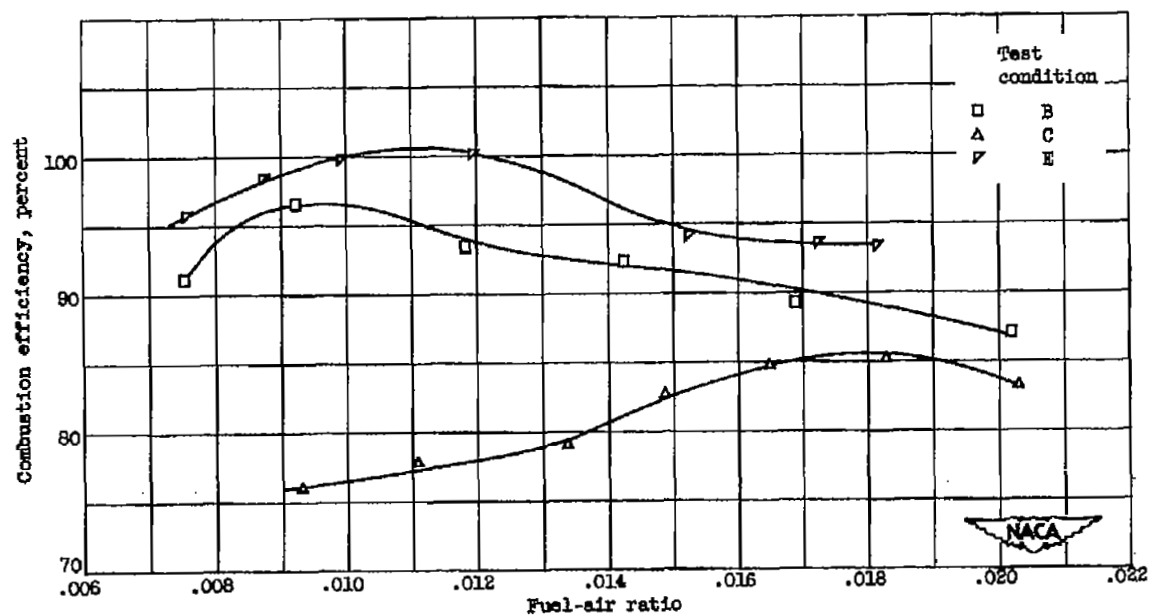


Figure 20. - Combustor pressure losses at test condition C.



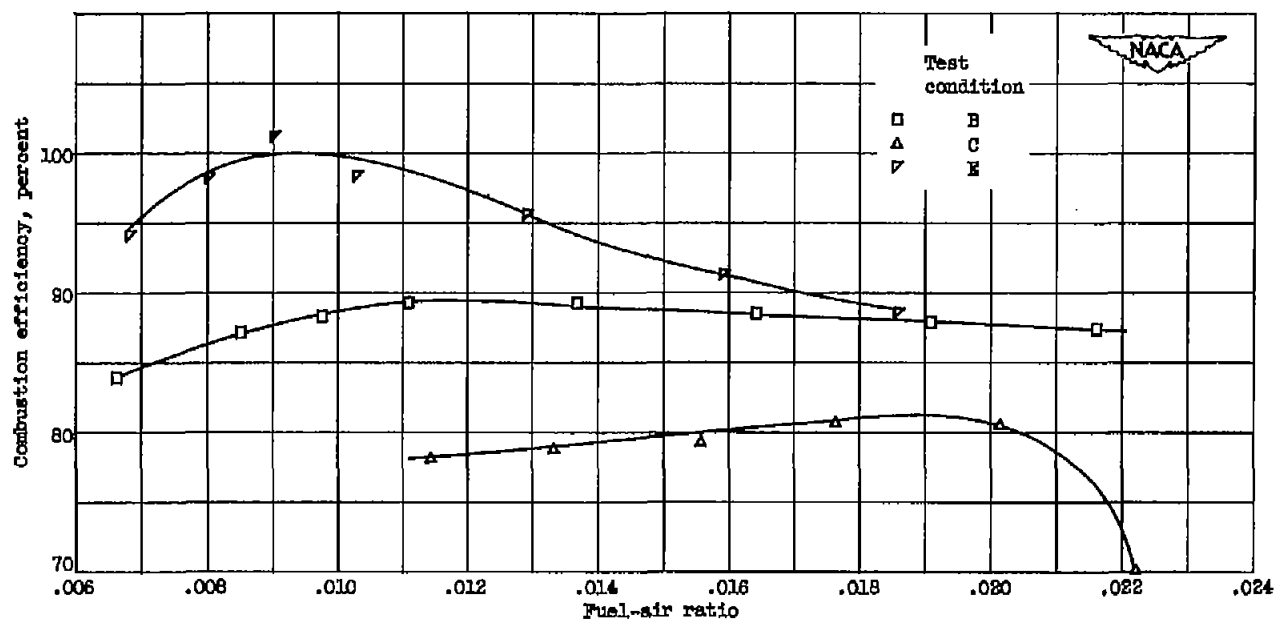
(a) Models 13B and 13C.

Figure 21. - Combustion efficiency of model 13 combustor with various fuel injectors.



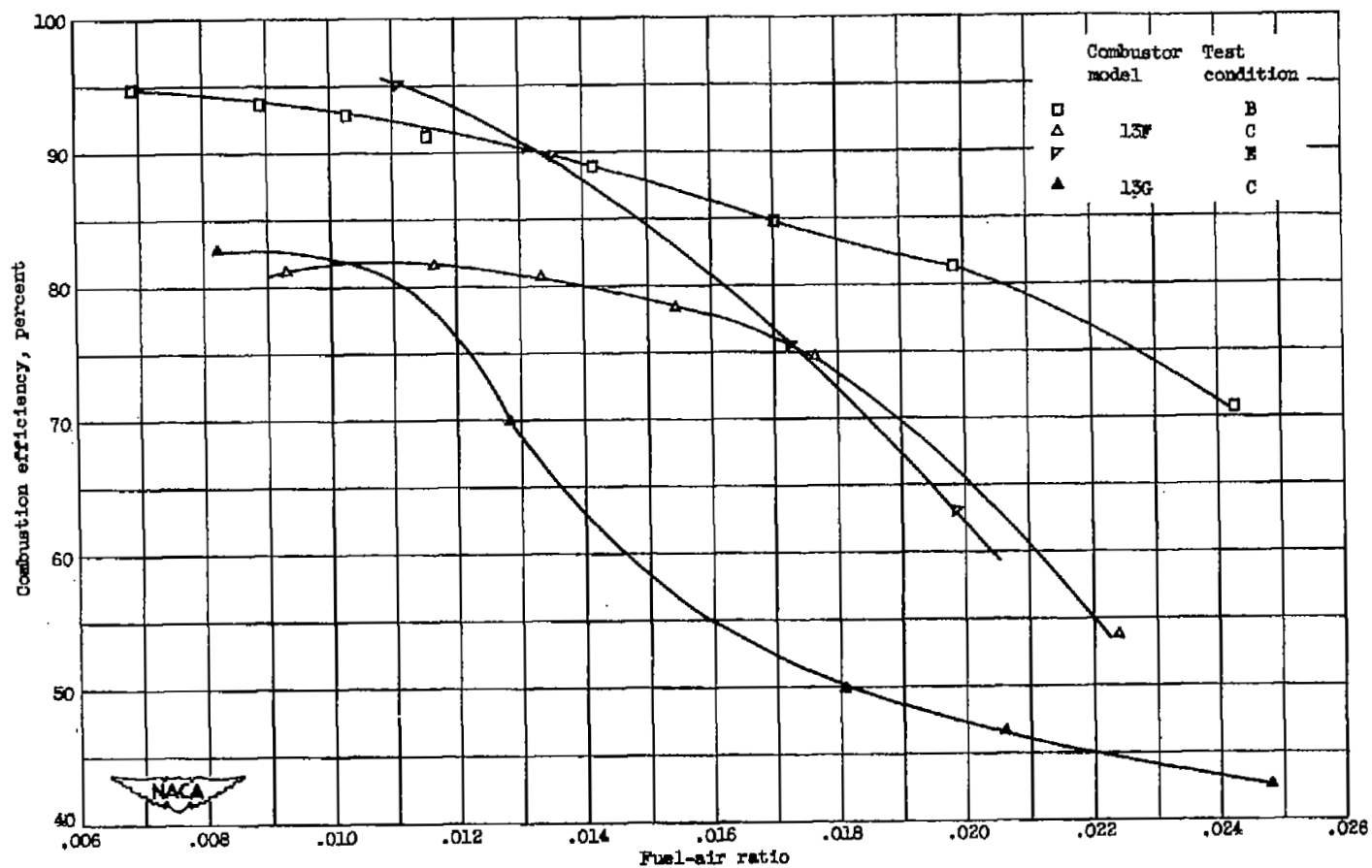
(b) Model 13D.

Figure 21. - Continued. Combustion efficiency of model 13 combustor with various fuel injectors.



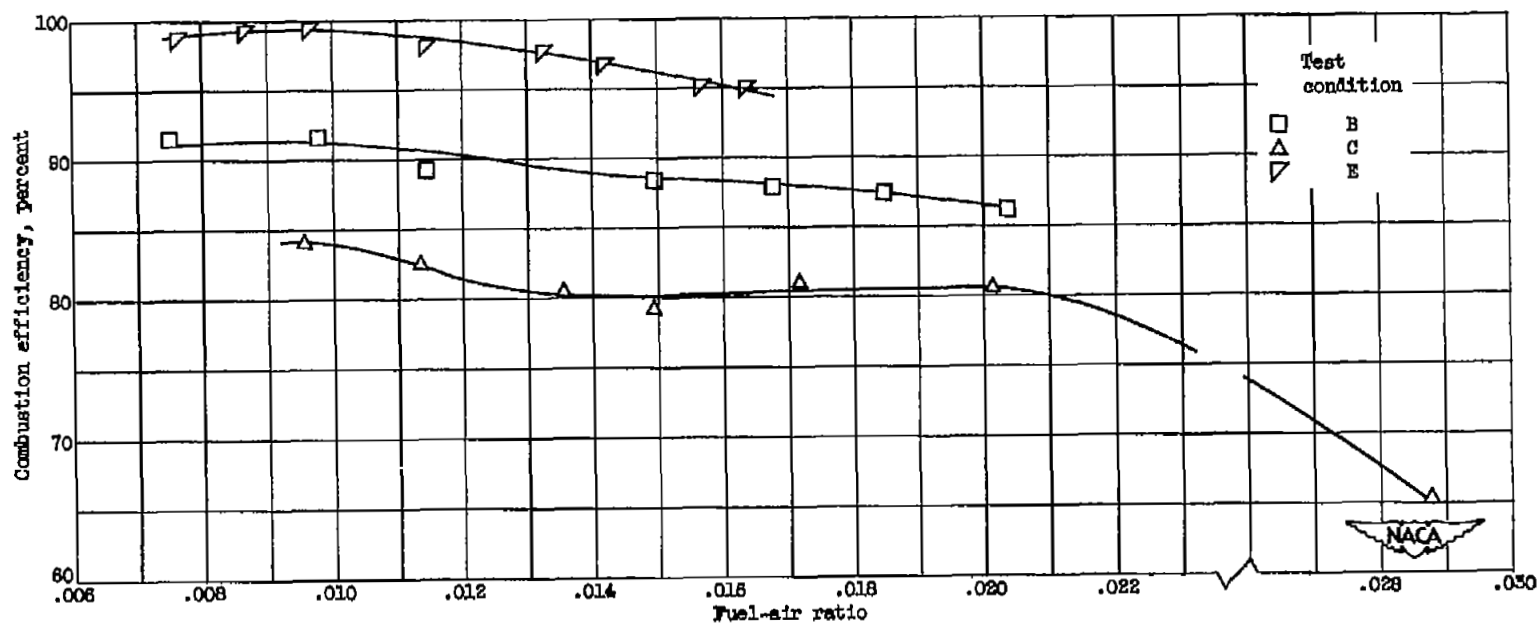
(c) Model 13E.

Figure 21. - Continued. Combustion efficiency of model 13 combustor with various fuel injectors.



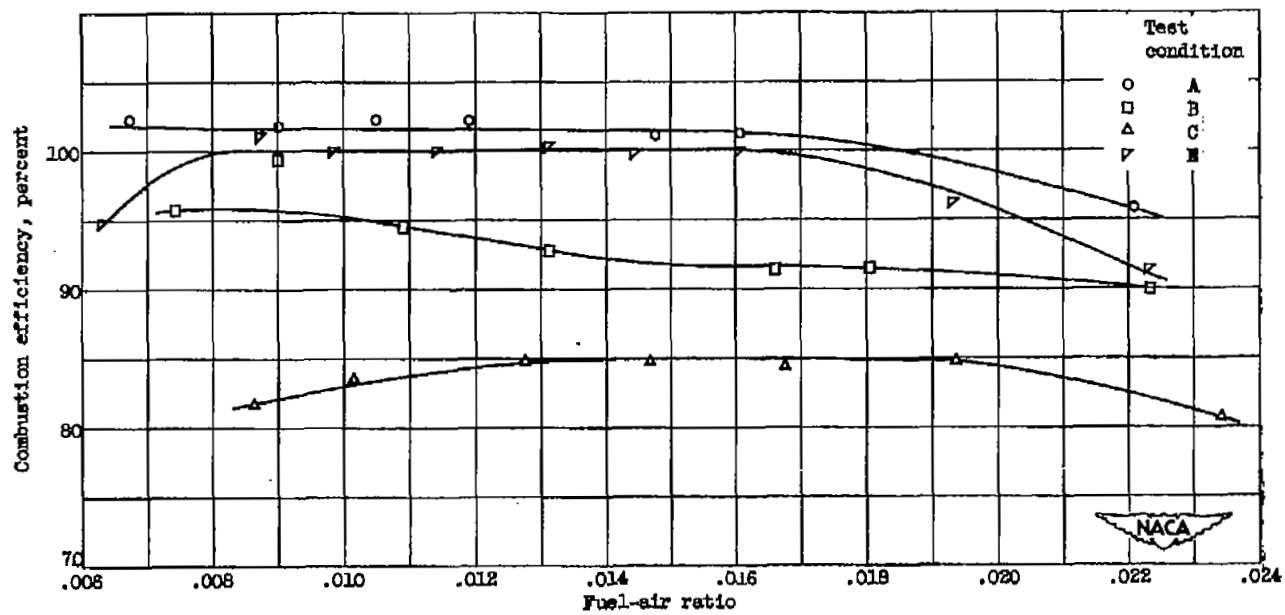
(d) Models 13F and 13G.

Figure 21. - Continued. Combustion efficiency of model 13 combustor with various fuel injectors.



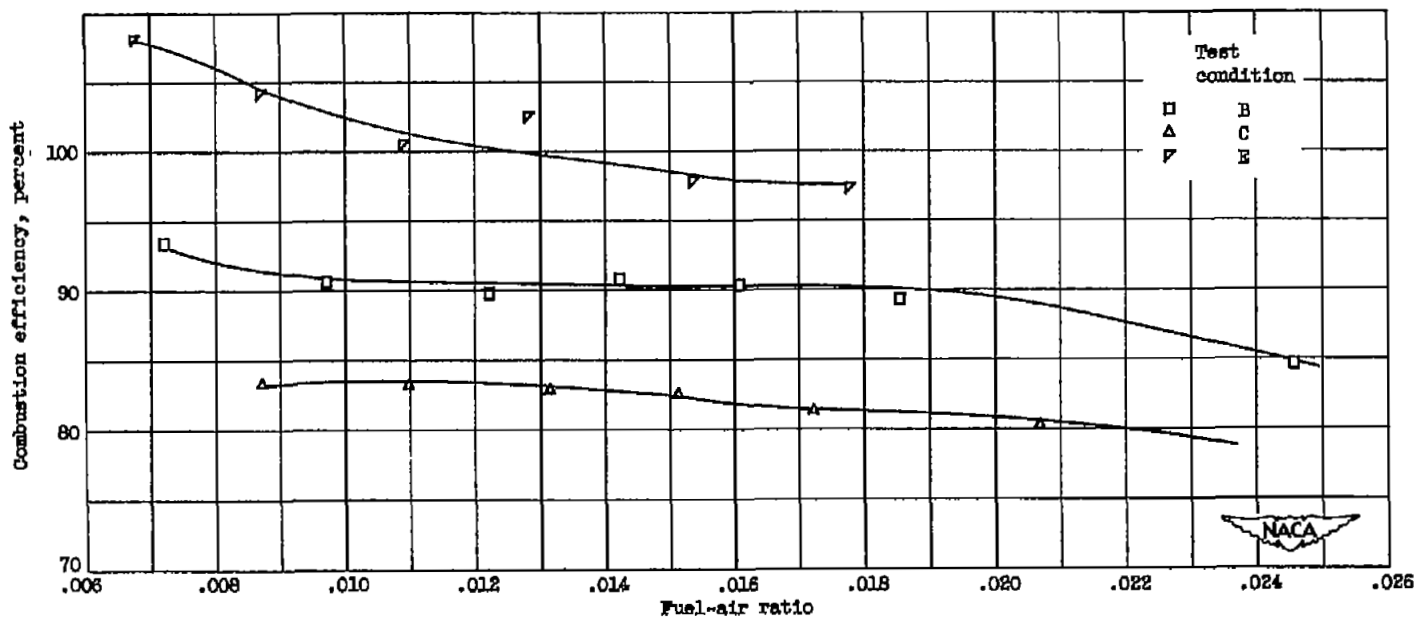
(e) Model 15H.

Figure 21. - Continued. Combustion efficiency of model 15 combustor with various fuel injectors.



(f) Model 13I.

Figure 21. - Continued. Combustion efficiency of model 13 combustor with various fuel injectors.



(g) Model 13J.

Figure 21. - Concluded. Combustion efficiency of model 13 combustor with various fuel injectors.

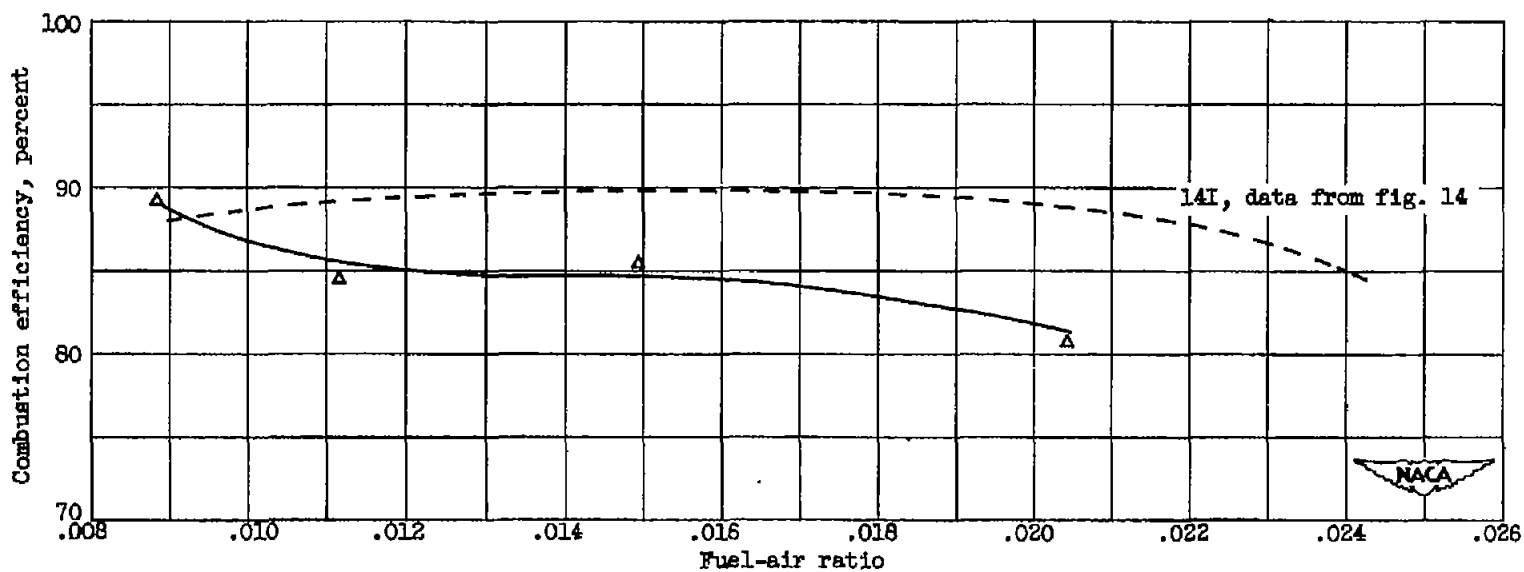


Figure 22. - Combustion efficiency of model 14K combustor at test condition C.

SECURITY INFORMATION

[REDACTED]

NASA Technical Library



3 1176 01435 6779

[REDACTED]